

When do Lyapunov Subcenter Manifolds become Eigenmanifolds? ^{*}

Yannik P. Wotte ^a, Arne Sachtler ^{b,c}, Alin Albu-Schäffer ^{b,c}, Stefano Stramigioli ^a,
Cosimo Della Santina ^{d,c}

^a*Robotics and Mechatronics, University of Twente (UT), Drienerlolaan 5, 7522 NB Enschede, Netherlands*

^b*Technical University of Munich (TUM), Munich, Germany*

^c*Institute of Robotics and Mechatronics, German Aerospace Center (DLR), Oberpfaffenhofen, Germany*

^d*Cognitive Robotics Department, Delft University of Technology (TU Delft), Netherlands*

Abstract

Multi-body mechanical systems have rich internal dynamics, which can be exploited to formulate efficient control targets. For periodic regulation tasks in robotics applications, this motivated the extension of the theory on nonlinear normal modes to Riemannian manifolds, and led to the definition of Eigenmanifolds. This definition is geometric, which is advantageous for generality within robotics but also obscures the connection of Eigenmanifolds to a large body of results from the literature on nonlinear dynamics. We bridge this gap, showing that Eigenmanifolds are instances of Lyapunov subcenter manifolds (LSMs), and that their stronger geometric properties with respect to LSMs follow from a time-symmetry of conservative mechanical systems. This directly leads to local existence and uniqueness results for Eigenmanifolds. Furthermore, we show that an additional spatial symmetry provides Eigenmanifolds with yet stronger properties of Rosenberg manifolds, which can be favorable for control applications, and we present a sufficient condition for their existence and uniqueness. These theoretical results are numerically confirmed on two mechanical systems with a non-constant inertia tensor: a double pendulum and a 5-link pendulum.

Key words: Nonlinear Dynamics, Multi-body mechanics, Eigenmanifolds, Symmetries, Differential Geometry

1 Introduction

Practical advances in robotics are pushing the need for a deeper understanding of the nonlinear dynamic behavior of multibody mechanical systems [1, 2, 3]. For example, a key challenge on the frontier of robotics lies in enabling robots to move efficiently while performing periodic motions (e.g., repetitive industrial operations, locomotion), thus avoiding motor torque limits and miti-

gating limited battery capacity [4, 5, 6, 7, 8]. An increasingly large body of literature looks at this challenge as exciting internal robot dynamics for low-torque control implementations, with modal analysis serving as the basis for these analyses [9, 10, 11, 12, 13].

Robots are usually multibody systems whose configuration is modeled to evolve on Riemannian manifolds with curvature [14]. As such, they are characterized by configuration-dependent inertia tensors, and they possess nonlinear and often chaotic open-loop dynamics [15]. This makes the direct application of the classic (nonlinear) modal theory challenging [16, 17, 18].

Eigenmanifolds have been recently introduced (see [19, Sec. 7]) as an extension of modal analysis to multi-body systems, in a way that naturally lends itself to control applications. Taking a geometric approach, these objects are defined starting from an equilibrium of conservative mechanical systems as two-dimensional submanifolds of the state space that collect periodic trajectories that ful-

^{*} This work is supported by the Advanced Grant M-Runner (Grant Agreement No. 835284) by the European Research Council (ERC).

This work is supported by the Advanced Grant PortWings (Grant Agreement No. 787675) by the ERC.

Email addresses: y.p.wotte@utwente.nl (Yannik P. Wotte), arne.sachtler@dlr.de (Arne Sachtler), alin.albu-schaeffer@tum.de (Alin Albu-Schäffer), s.stramigioli@utwente.nl (Stefano Stramigioli), cosimodellasantina@gmail.com (Cosimo Della Santina).

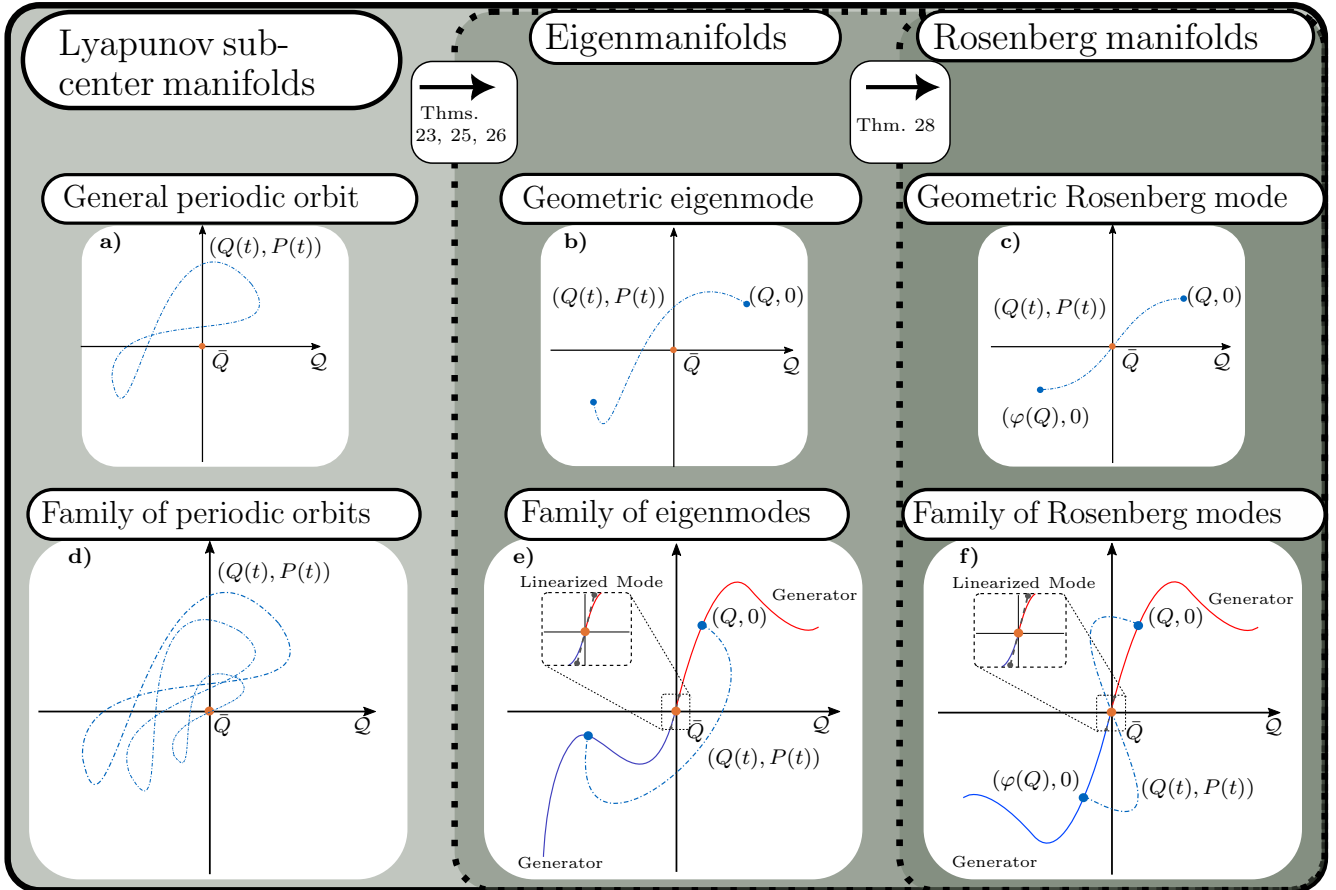


Figure 1. Summary of the article: (weak) Eigenmanifolds and (weak) Rosenberg manifolds are families of oscillations that arise in conservative mechanical systems. They are instances of Lyapunov subcenter manifolds, but they have stronger properties. Lyapunov subcenter manifolds (panel **d**) are families of general periodic modes (panel **a**). Instead, (weak) Eigenmanifolds (**e**) are families of (weak) geometric eigenmodes (**b**). We show that the existence of (weak) Eigenmanifolds is guaranteed by Theorems 23, 25 and 26. The existence of (weak) Rosenberg manifolds (**f**), which collect geometric Rosenberg modes (**c**) is guaranteed if, additionally, the conditions for Theorem 28 hold. In the present article, such (weak) Rosenberg manifolds have additional symmetry properties, which make them invariant under some $\varphi : \mathcal{Q} \rightarrow \mathcal{Q}$ specified in the article.

fill the properties of geometric eigenmodes (see also Figure 1). The definition (given in Section 2) is geometric which ensures broad applicability within robotics, particularly for systems with non-Euclidean configuration spaces (see also Figure 2). Eigenmanifolds are also immediately relevant as collections of promising control targets.

However, the geometric definition of Eigenmanifolds has obscured their connection to a large body of results in the nonlinear dynamics literature. Also, basic properties such as existence, uniqueness, and smoothness are unknown for Eigenmanifolds. Learning about such features requires numerical simulation on a case-by-case basis [20, 21]. These issues are hampering further developments in robotics and nonlinear control, so they need to be addressed.

In this paper, we make a first substantial step in this direction by deriving Eigenmanifolds as a sub-class of the more general Lyapunov subcenter manifolds (LSMs). Given a dynamical system $\dot{x} = f(x)$ with a conserved

quantity $H(x)$ (i.e., $\dot{H} = 0$), LSMs are two-dimensional submanifolds of the state-space that originate at equilibria with imaginary eigenvalues and collect periodic trajectories [22]. LSMs have been heavily investigated over the past decades [23, 24, 25] and have found important applications to disparate scenarios [26, 27, 28]. Contrary to Eigenmanifolds, LSMs are well-studied: there are results on existence, uniqueness, differentiability [29, 30], and persistence under dissipative disturbances [31] in the form of subspectral manifolds.

The theory of LSMs directly applies to conservative mechanical systems (i.e., including conservative multi-body mechanical systems, the domain of Eigenmanifolds), for which the Hamiltonian

$$H(Q, P) = \frac{1}{2}M(Q)^{-1}(P, P) + V(Q) \quad (1)$$

is the conserved quantity – where we used $Q \in \mathcal{Q}, P \in T_Q^*\mathcal{Q}$ to denote abstract configuration and momentum

variables, denote as $M(Q) \in \text{Symm}_+ T_{2,Q}^0 \mathcal{Q}$ the symmetric, positive-definite inertia tensor, and $V : \mathcal{Q} \rightarrow \mathbb{R}$ the potential energy.

Although not pointed out previously, Eigenmanifolds are clearly also LSMs. However, there are no conditions on the periodic trajectories collected in LSMs, and it is unknown when an LSM is an Eigenmanifold, and how the stronger properties of Eigenmanifolds arise.

Our contribution utilizes the time-symmetry $(Q, P, t) \rightarrow (Q, -P, -t)$ inherent to conservative mechanical systems to show that unique LSMs are (weak) Eigenmanifolds, thus inheriting existence & uniqueness to Eigenmanifolds, and we show that the stronger geometric properties of Eigenmanifolds follow from this symmetry. This successfully connects Eigenmanifolds to a large body of literature, opening future alleys for research on persistence under dissipation and bifurcations of Eigenmanifolds, with applications to control of multi-body systems.

Furthermore, we show that an additional spatial symmetry $(Q, P, t) \rightarrow (\sigma(Q, P), t)$ gives Eigenmanifolds the stronger properties of Rosenberg manifolds [19], also defined in Section 2 (see also Figure 1). These structures have further desirable control properties [32], and we provide a sufficient condition in terms of the inertia-tensor and potential energy function for the existence of Rosenberg manifolds. The condition we present is geometric, but we also show that it is equivalent to the existence of suitable local coordinates q, p where the equilibrium is $q = 0$, and the inertia matrix $M(q) \in \mathbb{R}^{n \times n}$ and the potential energy $V(q) \in \mathbb{R}$ satisfy $M(q) = M(-q)$ and $V(q) = V(-q)$. Such conditions may allow to shape Eigenmanifolds into Rosenberg manifolds at a design stage, and to investigate the shaping of Eigenmanifolds via inertial properties of robotic systems.

In summary, our contributions are:

- (1) Definitions 3, 7, 4 and 8 of weak geometric eigenmodes, weak geometric Rosenberg modes, weak Eigenmanifolds and weak Rosenberg manifolds
- (2) Theorem 6, stating that a so-called generator is guaranteed for weak Eigenmanifolds and weak Rosenberg manifolds
- (3) Existence and uniqueness of weak Eigenmanifolds descending from existence and uniqueness of LSMs via Theorem 25, which states that LSMs of conservative mechanical systems are weak Eigenmanifolds, if they are unique
- (4) Existence and uniqueness of Eigenmanifolds via Theorem 26, stating that LSMs in conservative mechanical systems are Eigenmanifolds, if they are unique and the configuration space is two-dimensional
- (5) Existence and uniqueness of weak Rosenberg manifolds via Theorem 28, a sufficient condition for (weak) Eigenmanifolds to exhibit the stronger properties of (weak) Rosenberg manifolds, respectively

The rest of the paper is organized as follows. First, a brief state of the art concludes this introductory section. Sec. 2 introduces theory that lies at the core of this article, with a focus on discrete symmetry groups of dynamical systems [33] and main definitions from Eigenmanifold theory [19].

Sec 3 derives properties of orbits that are fixed sets of a symmetry. For periodic orbits in conservative mechanical systems, this is shown to recover properties of geometric eigenmodes and geometric Rosenberg modes.

Next, Sec. 4, derives the main theoretical contributions of this article. We prove that unique LSMs of conservative mechanical systems fulfill the stronger properties of Eigenmanifolds, and derive a sufficient condition for Eigenmanifolds to fulfill the stronger properties of Rosenberg manifolds.

Sec. 5 verifies the results in numerical examples of conservative mechanical systems, highlighting the existence of Eigenmanifolds and Rosenberg manifolds.

We end with a conclusion in Sec. 6. Proofs are given in Appendix A, and Appendix B contains background on LSMs and choice of coordinates.

1.1 Related literature

Exciting and exploiting efficient nonlinear oscillations is an open challenge in nonlinear control theory [34, 35, 36], with important ramifications in robotics' locomotion and execution of industrial operations [37, 38, 39, 40, 41], and biomechanics [42, 43, 44]. To this end, both design of mechanical systems [45] and shaping of Eigenmanifolds via the systems potential energy [46, 47] has been explored. Eigenmanifolds of interest are stabilized in simulation [48, 49], on real systems [50], can be stabilized in an energy-efficient manner [51] and allow the swing-up of weakly actuated systems to high energies [20]. Eigenmanifolds have also been applied in classifying the accuracy of reduced order models in soft robotics [52, 21].

Eigenmanifold theory has its precursors in the study of nonlinear normal modes [53, 18, 54] for nonlinear mechanical systems with constant inertia tensors. Rosenberg modes are well-studied for conservative mechanical systems [16, 17, 55], and their symmetry properties are known by the condition that $V(q) = V(-q)$. Strict normal modes are a special case of Eigenmanifolds that exist under compatibility of the potential gradient with the geodesic flow [56].

Within the nonlinear dynamics literature, LSMs are long studied [22, 29, 30] and their persistence in the limit of small dissipation was shown [31], but this has not been connected to insights about Eigenmanifolds in multi-body dynamics. LSMs have also been applied to the model order reduction of partial differential equations [57].

A general treatment of discrete symmetries in dynamical systems is given by Michael Field [58]. Large classes of symmetries were also studied in the context of peri-

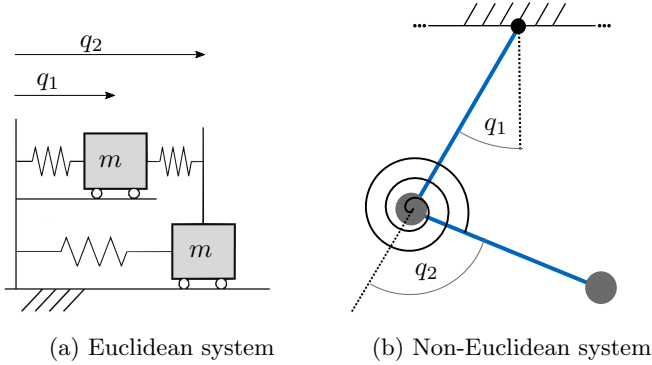


Figure 2. Examples of two simple mechanical systems with different inertia properties. The system of two masses in panel (a) has a Euclidean configuration space with a constant inertia tensor, while the double pendulum in panel (b) has a non-Euclidean configuration space with a non-zero curvature, such that the associated inertia tensor is non-constant in any choice of coordinates.

odic orbits and nonlinear normal modes [59, 60]. However, these works largely treat symmetries on vector and Banach spaces, and do not directly apply to Eigenmanifold theory. An excellent overview to time-reversal symmetries in Hamiltonian systems is given by Lamb and Roberts [61], covering many properties of direct relevance to Eigenmanifold theory, such as the existence of time-symmetric LSMs. Alomair and Montaldi [62] investigate the interplay of a time-reversal and a spatial symmetry of Hamiltonian systems in the context of periodic orbits, proving the existence of a discrete number of doubly symmetric periodic orbits around symmetric equilibria. However, both of [61, 62] leave properties of such symmetric orbits and their families implicit.

2 Preliminaries and problem statement

We briefly introduce discrete symmetries, Lyapunov subcenter manifolds, and Eigenmanifolds for Hamiltonian systems, and conclude with a formal problem statement.

2.1 Notation

Smooth manifolds are denoted $\mathcal{M}, \mathcal{N}, \mathcal{Q}$. At a point $m \in \mathcal{M}$, $T_m \mathcal{M}$ denotes the tangent space of \mathcal{M} at m , and $T_m^* \mathcal{M}$ denotes the respective cotangent space. The tangent bundle over \mathcal{M} is $T\mathcal{M}$, and the cotangent bundle is $T^*\mathcal{M}$. The set of vector fields over \mathcal{M} is $\Gamma(T\mathcal{M})$. For a smooth map $\sigma : \mathcal{M} \rightarrow \mathcal{N}$ between smooth manifolds \mathcal{M}, \mathcal{N} we write $\sigma \in C^\infty(\mathcal{M}, \mathcal{N})$. The pushforward of σ is $\sigma_* : T_p \mathcal{M} \rightarrow T_{\sigma(p)} \mathcal{N}$, and the pullback is $\sigma^* : T_{\sigma(p)}^* \mathcal{N} \rightarrow T_p^* \mathcal{M}$. The image of σ is denoted $\sigma(\mathcal{M}) := \{\sigma(m) \mid m \in \mathcal{M}\} \subseteq \mathcal{N}$. Additional symbols introduced in the paper are summarized in Table 1.

2.2 Lyapunov subcenter manifolds, Eigenmanifolds and Rosenberg manifolds

We describe conservative mechanical systems with configuration space \mathcal{Q} by their Hamiltonian dynamics on the cotangent bundle $T^*\mathcal{Q}$, where the Hamiltonian H in Equation (1) canonically determines the Hamiltonian vector field $X_H \in \Gamma(TT^*\mathcal{Q})$ (for details on the construction, see e.g., Bullo [14]). Let $\gamma : \mathbb{R} \rightarrow T^*\mathcal{Q}$ denote a solution to the abstract Hamiltonian dynamics

$$\dot{\gamma} = X_H(\gamma), \quad \gamma(0) = \gamma_0. \quad (2)$$

We further denote the flow of X_H as the map

$$\Psi_{X_H}^t : T^*\mathcal{Q} \rightarrow T^*\mathcal{Q}, \quad \gamma(t) = \Psi_{X_H}^t(\gamma_0), \quad (3)$$

where $\Psi_{X_H}^t$ is defined such that $\gamma(t) = \Psi_{X_H}^t(\gamma_0)$ solves (2). We assume that X_H is complete, which means that t can take values in all of \mathbb{R} . The set of points on $\gamma(t)$ is denoted $\gamma(\mathbb{R}) := \Psi_{X_H}^{\mathbb{R}}(\gamma_0) \subset \mathcal{M}$.

In a canonical chart (see Appendix B.2) with $q, p \in \mathbb{R}^n$ the dynamics (2) read

$$\dot{q} = \frac{\partial H}{\partial p}(q, p) = M(q)^{-1}p, \quad (4)$$

$$\begin{aligned} \dot{p} &= -\frac{\partial H}{\partial q}(q, p) \\ &= -\frac{\partial}{\partial q} \left(\frac{1}{2} p^\top M(q)^{-1} p \right) - \frac{\partial V}{\partial q}(q). \end{aligned} \quad (5)$$

We are interested in families of periodic oscillations springing from an isolated equilibrium of (4) (i.e., a point (q, p) with $p = 0$, $\frac{\partial V}{\partial q}(q) = 0$, and $\frac{\partial^2 V}{\partial q^2}(q) > 0$).

Definition 1 (Lyapunov subcenter manifold) *We call a 2-dimensional, invariant, connected submanifold $\mathfrak{M} \subset T^*\mathcal{Q}$ a Lyapunov subcenter manifold (LSM) if it collects periodic orbits, contains an equilibrium \bar{Q} and is tangent to a linear, 2-dimensional Eigenspace $E_0 \subset T_{(\bar{Q}, 0)} T^*\mathcal{Q}$ of (2).*

Theory for LSMs is general enough to be applied to systems of the form $\dot{x} = f(x)$, we merely present a mildly adapted form for systems on $T^*\mathcal{Q}$. Specifically, we focus on dynamical systems that read, in local coordinates with $x \in \mathbb{R}^{2n}$:

$$\dot{x} = Ax + B(x), \quad (6)$$

where $A \in \mathbb{R}^{2n \times 2n}$, and $B : \mathbb{R}^{2n} \rightarrow \mathbb{R}^{2n}$ is analytic and such that $B(0) = 0$, $\frac{\partial B}{\partial x}(0) = 0$. Details on the construction, existence and uniqueness are summarized in Appendix B.1. For a complete treatment, refer to de la Llave et al. [30, 31] and references therein.

There are no further conditions on trajectories collected

Table 1
Table of Symbols and Notation

Symbol	Description	Defined in
\mathcal{Q}	configuration manifold	Sec. 2.2
$T^*\mathcal{Q}$	cotangent bundle	Sec. 2.2
$\pi_{\mathcal{Q}} : T^*\mathcal{Q} \rightarrow \mathcal{Q}$	projection to configuration	Sec. 2.2
$Q \in \mathcal{Q}, P \in T_{\mathcal{Q}}^*\mathcal{Q}$	abstract configuration and momentum variables	Sec. 2.2
$q, p \in \mathbb{R}^n$	configuration and momentum in a canonical chart	Sec. B.2
$H : T^*\mathcal{Q} \rightarrow \mathbb{R}$	Hamiltonian	Sec. 1
$X_H \in \Gamma(TT^*\mathcal{Q})$	abstract Hamiltonian vector field	Sec. 2.2
$\gamma : \mathbb{R} \rightarrow T^*\mathcal{Q}$	abstract integral curve of X_H	Sec. 2.2
$x : \mathbb{R} \rightarrow \mathbb{R}^{2n}$	integral curve of X_H in a canonical chart	Sec. 3.1
$\lambda_0 \in \mathbb{C}$	Eigenvalue of linearized system	Sec. B.1
$E_0 \in T_{(\bar{Q}, 0)}T^*\mathcal{Q}$	Eigenspace of linearized system	Sec. B.1
$\mathfrak{M} \subset T^*\mathcal{Q}$	LSM, Eigenmanifold or Rosenberg manifold	Secs. 2.2, B.1
$\mathcal{R} \subset \mathfrak{M}$	generator of an Eigenmanifold	Sec. 2.2
$\phi_{\gamma} : [0, 1] \rightarrow \mathcal{Q}$	immersion or immersion of geometric Eigenmode γ	Sec. 2.2
$\tau \in \mathbb{R}$	time-scaling	Sec. 3.1
$\sigma : \mathcal{M} \rightarrow \mathcal{M}$	symmetry map	Sec. 3.1
$S : \mathbb{R}^n \rightarrow \mathbb{R}^n$	coordinate version of symmetry map	Sec. 3.1
$\text{Fix}(\sigma)$	fixed set of a symmetry	Sec. 3.1
$\Psi_f^t : \mathcal{M} \rightarrow \mathcal{M}$	Flow of $f \in \Gamma(T\mathcal{M})$	Sec. 3.1

within an LSM (see e.g., Figure 1a). This is different for Eigenmanifolds, which collect geometric eigenmodes (see Figure 1b), whose definition demands additional structure. Eigenmanifolds are defined on tangent or cotangent bundles. We cover the case for cotangent bundles (for the tangent bundle case, see Remark 5). First, define the projection of the cotangent bundle $T^*\mathcal{Q}$ to the configuration manifold \mathcal{Q} as

$$\pi_{\mathcal{Q}} : T^*\mathcal{Q} \rightarrow \mathcal{Q}, (Q, P) \mapsto Q. \quad (7)$$

Then, the definition of a geometric eigenmode is

Definition 2 (Geometric Eigenmode) *Given a T -periodic oscillation $\gamma : \mathbb{R} \rightarrow T^*\mathcal{Q}$, it is called a geometric eigenmode if $\pi_{\mathcal{Q}}(\gamma(\mathbb{R})) \cong [0, 1]$, i.e., there is an embedding $\phi_{\gamma} : [0, 1] \rightarrow \mathcal{Q}$ such that $\phi_{\gamma}([0, 1]) = \pi_{\mathcal{Q}}(\gamma(\mathbb{R}))$.*

For geometric eigenmodes, the set $\pi_{\mathcal{Q}}(\gamma(\mathbb{R}))$ is homeomorphic to a line segment, i.e., it does not self-intersect (see Figure 1b). A weaker definition allows for self-intersections (see Figure 3a) by allowing that ϕ_{γ} is an immersion, rather than an embedding. While an embedding is injective, an immersion has the weaker requirement that only the pushforward $\phi_{\gamma*}$ has to be injective.

Definition 3 (Weak Geometric Eigenmode) *Given a T -periodic oscillation $\gamma : \mathbb{R} \rightarrow T^*\mathcal{Q}$, it is*

called a weak geometric eigenmode if there is an immersion $\phi_{\gamma} : [0, 1] \rightarrow \mathcal{Q}$ ¹ with $\phi_{\gamma}(0) \neq \phi_{\gamma}(1)$, such that $\phi_{\gamma}([0, 1]) = \pi_{\mathcal{Q}}(\gamma(\mathbb{R}))$.

Note that both geometric and weak geometric eigenmodes contain two points with $P = 0$, namely the endpoints $\phi_{\gamma}(0)$ and $\phi_{\gamma}(1)$. As such, both are instances of periodic brake trajectories [63], but with stronger properties that are the focus of our article. A (weak) Eigenmanifold is then defined as a collection of (weak) geometric eigenmodes:

Definition 4 ((Weak) Eigenmanifold) *A 2-dimensional invariant, connected sub-manifold $\mathfrak{M} \subseteq T^*\mathcal{Q}$ is an Eigenmanifold if all trajectories contained within it are (weak) geometric eigenmodes, it contains an equilibrium Q and is tangent to a linear, 2-dimensional Eigenspace $E_0 \subset T_{(Q, 0)}T^*\mathcal{Q}$.*

Remark 5 *The definition of [19, Sec. 7] uses a Lagrangian formalism, where Eigenmanifolds $\mathfrak{M} \subset T\mathcal{Q}$ are*

¹ The interval $[0, 1]$ is a manifold with boundary, for which the notion of an immersion is not immediately defined. An immersion $\sigma : \mathcal{M} \rightarrow \mathcal{N}$ for a manifold \mathcal{M} with boundary $\partial\mathcal{M}$ is defined such that $\sigma|_{\partial\mathcal{M}}$ is an immersion of $\partial\mathcal{M}$. For $\mathcal{M} = [0, 1]$, the boundary is $\partial\mathcal{M} = \{0, 1\}$. Since this boundary is 0-dimensional it has no tangent-space, and any map classifies as an immersion for it.

considered subsets of the tangent bundle TQ . For the considered mechanical systems a Hamiltonian formalism with $\mathfrak{M} \subset T^*Q$ is equally applicable, since the invertible inertia tensor defines a bijection $M : TQ \rightarrow T^*Q$.

An important object in the context of Eigenmanifolds is the generator $\mathcal{R} \subset \mathfrak{M}$, which is next shown to be a 1D connected submanifold that collects points $(Q, 0)$, called brake points, of the geometric eigenmodes:

Theorem 6 (Existence of generator) *Given a smooth Eigenmanifold \mathfrak{M} that satisfies Definition 4, the set $\mathcal{R} := \{(Q, 0) \mid (Q, 0) \in \mathfrak{M}\}$ is a connected, 1D submanifold containing the equilibrium and $\mathfrak{M} = \Psi_{X_H}^{\mathbb{R}}(\mathcal{R})$, i.e., \mathcal{R} generates \mathfrak{M} .*

PROOF. See Appendix A.1 Prior definitions of Eigenmanifolds [19, Sec. 7] explicitly assumed the existence of the generator - but we conclude from Theorem 6 that this assumption is not necessary.

Next we define Rosenberg manifolds, which have yet stronger properties. As with Eigenmanifolds, Rosenberg manifolds are defined on tangent or cotangent bundles. We first define (weak) geometric Rosenberg modes (see also Figure 3b).

Definition 7 ((Weak) Geometric Rosenberg Mode)

*A T -periodic oscillation $\gamma : \mathbb{R} \rightarrow T^*Q$ is a (weak) geometric Rosenberg mode with respect to an equilibrium \bar{Q} if it is both a (weak) geometric eigenmode, and $\bar{Q} \in \pi_Q(\gamma(\mathbb{R}))$, i.e., if γ passes through the equilibrium configuration \bar{Q} for some momentum P .*

Finally, define the Rosenberg manifold [19, Sec. 7] as an Eigenmanifold of geometric Rosenberg modes:

Definition 8 ((Weak) Rosenberg Manifold)

*An Eigenmanifold $\mathfrak{M} \subseteq T^*Q$ is a Rosenberg manifold if it admits a generator, and all trajectories contained within it are (weak) Rosenberg modes.*

2.3 Problem statement

It is at this point clear, albeit not recognized before this work, that Eigenmanifolds and Rosenberg manifolds of conservative mechanical systems are Lyapunov subcenter manifolds. This work asks the converse question:

When is a Lyapunov subcenter manifold of a conservative mechanical system an Eigenmanifold, and when is it also a Rosenberg manifold?

3 Symmetries of conservative mechanical systems

In this section we introduce a well-known time symmetry and generalize an often-used spatial symmetry of

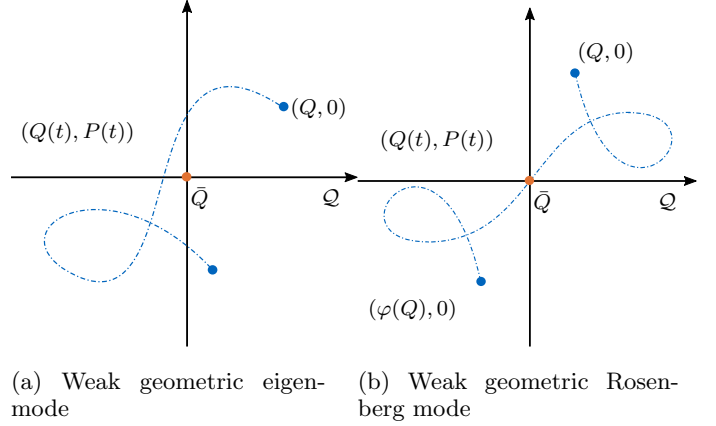


Figure 3. Example of a weak geometric eigenmode in panel (a) and a (φ -equivariant, see Section 3) weak geometric Rosenberg mode in panel (b). Extending their non-weak counterparts, respectively, these allow for self-intersections in configuration space.

Hamiltonian systems, and derive properties of trajectories subject to these symmetries. The results will be instrumental to showing stronger properties of LSMs in conservative mechanical systems, in Section 4.

3.1 Symmetries

We begin by defining the concept of a symmetry. For a general treatment of symmetries of Hamiltonian systems see e.g., [61, 62].

Definition 9 (Symmetry) *A symmetry (σ, τ) of the dynamics $f \in \Gamma(TM)$ consists of a diffeomorphism $\sigma : \mathcal{M} \rightarrow \mathcal{M}$ and a time-scaling $\tau \in \{-1, 1\}$ such that*

$$f \circ \sigma = \tau \sigma_* f. \tag{8}$$

Symmetries map solutions to solutions, where we present a geometric version of a known theorem (e.g., [33]):

Theorem 10 (Symmetry mapping of solutions)

Given a vector field $f \in \Gamma(TM)$, a diffeomorphism $\sigma : \mathcal{M} \rightarrow \mathcal{M}$ and a time-scaling $\tau \in \{-1, 1\}$, then Equation (8) is equivalent to:

$$\Psi_f^t(\sigma(m)) = \sigma(\Psi_f^{\tau t}(m)). \tag{9}$$

Remark 11 *Given a local chart (U, X) with $m, \sigma(m) \in U \subset \mathcal{M}$ and chart map $X : U \subset \mathcal{M} \rightarrow \mathbb{R}^n$, the vector field f is represented as $F : \mathbb{R}^n \rightarrow \mathbb{R}^n$ by $F = X_* f \circ X^{-1}$, and the symmetry as $S : \mathbb{R}^n \rightarrow \mathbb{R}^n$ by $S = X \circ \sigma \circ X^{-1}$. Then condition (8) reads*

$$F(S(x)) = \tau \frac{\partial S}{\partial x} F(x), \tag{10}$$

and both $x(t)$ and $S(x(\tau t))$ are solutions of the dynamics $\dot{x} = F(x)$.

Finally, we define the set \mathcal{O}_f^σ of orbits of f that are fixed under a symmetry (σ, τ) as

$$\mathcal{O}_f^\sigma := \{\Psi_f^\mathbb{R}(m) \mid \Psi_f^\mathbb{R}(m) = \sigma \Psi_f^\mathbb{R}(m)\}, \quad (11)$$

and define the fixed orbit subset $\text{Fix}(\sigma) \subset \mathcal{M}$ as the union of the orbits in \mathcal{O}_f^σ

$$\text{Fix}(\sigma) := \bigcup_{\gamma \in \mathcal{O}_f^\sigma} \gamma(\mathbb{R}). \quad (12)$$

3.2 Time reversal symmetry

The equations of motion of a conservative mechanical system with Hamiltonian dynamics 2 are subject to the time-reversal symmetry $(Q, P, t) \rightarrow (Q, -P, -t)$. As shown by [61], this follows more generally for any Hamiltonian system when $H(Q, P) = H(Q, -P)$. Following Definition 9, we write this as (σ_1, τ_1) , with

$$\sigma_1((Q, P)) = (Q, -P), \quad \tau_1 = -1. \quad (13)$$

By an application of Theorem 10, the presence of this symmetry means that if an evolution $\gamma(t) = (Q(t), P(t))$ is a solution of (2), then $\delta(t) = (Q(-t), -P(-t))$ is also a solution of (2). In this subsection, we are interested in trajectories whose orbits are fixed sets of the symmetry, i.e., $\gamma(\mathbb{R}) \in \text{Fix}(\sigma_1)$, or equivalently

$$\gamma(\mathbb{R}) = \sigma_1(\gamma(\mathbb{R})), \quad (14)$$

and we show that these orbits satisfy the properties of geometric eigenmodes.

Theorem 12 (Thm. 4.1, [61]) *Given Hamiltonian dynamics with $H(Q, P) = H(Q, -P)$.*

(a) *An evolution $\gamma(t) = (Q(t), P(t))$ of (2) satisfies*

$$\gamma(\mathbb{R}) = \sigma_1(\gamma(\mathbb{R})). \quad (15)$$

if and only if there is t' such that $P(t') = 0$.

(b) *Given $T > 0$, a T -periodic orbit $(Q(t), P(t))$ (i.e., $(Q(t), P(t)) = (Q(t + T), P(t + T))$) encounters either 0 or 2 distinct points with $P(t) = 0$.*

PROOF. This directly follows from Theorem 4.1a in [61] with $\text{Fix}(\sigma_1) = \mathcal{Q} \times 0 \subset T^*\mathcal{Q}$, i.e., the fixed set of the symmetry σ_1 is the zero section of $T^*\mathcal{Q}$. An intuitive explanation of Theorem 12 goes as follows: by Theorem 12a, any trajectory $(Q(t), P(t))$ with $P(0) = 0$ satisfies:

$$Q(t) = Q(-t). \quad (16)$$

i.e., the backwards and forwards evolution of the configuration from a starting point $(Q(0), 0)$ are identical -

visually speaking, points with $P = 0$ appear to reflect $Q(t)$. If the orbit is also periodic, $Q(t)$ that satisfies (16) must be reflected at a second point with $P = 0$. There can be no further reflections in between, leading to the condition that either zero or two points with $P = 0$ are encountered. This is captured in Theorem 12b.

Lemma 13 *Given an evolution $\gamma(t) = (Q(t), P(t))$ of (2). If there are two distinct points $(Q_1, 0), (Q_2, 0) \in \gamma(\mathbb{R})$ and denoting $\Delta t = \min\{t > 0 \mid (Q_2, 0) = \Psi_{X_H}^t(Q_1, 0)\}$, then the evolution is periodic with period $T = 2\Delta t$.*

PROOF. See Appendix A.3.

Corollary 14 *To each Eigenmanifold \mathfrak{M} are associated exactly two generators \mathcal{R} intersecting at the equilibrium.*

PROOF. The Corollary directly follows from Theorem 6 asserting the existence of one generator, and Theorem 12b. Since a generator is a collection of states with zero momentum, each lying on periodic orbits contained in \mathfrak{M} , Theorem 12b asserts a second point of zero momentum for each point on the generator. By continuity of the flow map, such second points are collected on a second generator.

Corollary 15 *Given $T > 0$, a T -periodic orbit $\gamma(t)$ is a weak geometric eigenmode if and only if it satisfies the symmetry*

$$\gamma(\mathbb{R}) = \sigma_1(\gamma(\mathbb{R})). \quad (17)$$

PROOF. See Appendix A.3.

3.3 Equivariant symmetry

Given a diffeomorphism $\varphi : \mathcal{Q} \rightarrow \mathcal{Q}$, we present conditions for the presence of an equivariant symmetry $(Q, P, t) \rightarrow (\varphi(Q), (\varphi^{-1})^*P, t)$. We write this as (σ_2, τ_2) with

$$\sigma_2((Q, P)) = (\varphi(Q), (\varphi^{-1})^*P), \quad \tau_2 = 1. \quad (18)$$

We further restrict our attention to φ that leaves the equilibrium $\bar{Q} \in \mathcal{Q}$ fixed, and which satisfies that $\varphi_*(\bar{Q}) = -\text{id}_{T_{\bar{Q}}\mathcal{Q}}$, and $\varphi \circ \varphi = \text{id}_{\mathcal{Q}}$. It is shown in Appendix A that this symmetry applies to conservative mechanical systems (4), when the inertia tensor and the potential field are simultaneously even symmetric about \bar{Q} , i.e., $M = \varphi^*M$ and $V = V \circ \varphi$. The conditions guarantee that a local chart exists (see Appendix B.4) that maps \bar{Q} to $q = 0$, and where the symmetry reads $(q, p, t) \rightarrow (-q, -p, t)$, such that (σ_2, τ_2) can be written as (S_2, τ_2) with

$$S_2((q, p)) = (-q, -p), \quad \tau_2 = 1. \quad (19)$$

In such coordinates the conditions on M and V read $M(q) = M(-q)$ and $V(q) = V(-q)$. We refer to these coordinates as φ -equivariant coordinates. In this subsection, we are interested in trajectories whose orbits are fixed sets of the symmetry (σ_2, τ_2) , i.e., $\gamma(\mathbb{R}) \in \text{Fix}(\sigma_2)$ or

$$\gamma(\mathbb{R}) = \sigma_2(\gamma(\mathbb{R})), \quad (20)$$

and orbits that are fixed sets of both (σ_1, τ_1) and (σ_2, τ_2) , i.e., $\gamma(\mathbb{R}) \in \text{Fix}(\sigma_1) \cap \text{Fix}(\sigma_2)$ or

$$\gamma(\mathbb{R}) = \sigma_1(\gamma(\mathbb{R})) = \sigma_2(\gamma(\mathbb{R})), \quad (21)$$

and we show that latter orbits satisfy the properties of geometric Rosenberg modes. The corresponding results are collected in Lemma 16 and Lemma 18.

Lemma 16 *Given an evolution $\gamma(t) = (Q(t), P(t))$ of (2). If there is a pair of points $(Q, P), (\varphi(Q), \varphi^{-1*}P) \in \gamma(\mathbb{R})$ and denoting $\Delta t = \min\{t > 0 \mid (\varphi(Q), \varphi^{-1*}P) = \Psi_{X_H}^t((Q, P))\}$, then the evolution is periodic with period $T = 2\Delta t$ and*

$$\gamma(\mathbb{R}) = \sigma_2(\gamma(\mathbb{R})). \quad (22)$$

PROOF. See Appendix A.3.

Remark 17 *In φ -equivariant coordinates, Lemma 16 holds if there is a pair of points $(q, p), (-q, -p) \in \gamma(\mathbb{R})$.*

Lemma 18 *Given an evolution $\gamma(t) = (Q(t), P(t))$ of (2). If there is a pair of points $(Q, 0), (\varphi(Q), 0) \in \gamma(\mathbb{R})$ then $\nu \in \mathbb{R}^n$ exists such that $(\mathbf{q}, \nu) \in \gamma(\mathbb{R})$, with $\mathbf{q} = \varphi(\mathbf{q})$.*

PROOF. See Appendix A.3.

Remark 19 *A fixed point is necessarily an equilibrium [33], but Lemma 18 only guarantees the solution $\gamma(t)$ to pass through a particular fixed point if it is unique.*

Corollary 20 *Given $T > 0$, a T -periodic orbit $\gamma(t)$ is a weak geometric Rosenberg mode if it satisfies the symmetries*

$$\gamma(\mathbb{R}) = \sigma_1(\gamma(\mathbb{R})) = \sigma_2(\gamma(\mathbb{R})). \quad (23)$$

If the fixed point \bar{Q} of σ_1, σ_2 is the only fixed point such that $V(\bar{Q}) < V(Q)$ for $(Q, 0) \in \gamma(\mathbb{R})$, then $\gamma(t)$ is a weak geometric Rosenberg mode w.r.t. \bar{Q} .

PROOF. See Appendix A.3.

4 From LSMs to Eigenmanifolds and Rosenberg manifolds

This section presents our main results, combining the symmetries introduced in Sec. 3 with modal theory on Lyapunov subcenter manifolds.

4.1 Propagation of symmetries

Theorem 21, presented hereafter, is a novel result that is essential to derive results in the remainder of this section. Given a symmetry (σ, τ) of $f(x)$, it presents conditions for an LSM \mathfrak{M} and trajectories contained within it to be fixed sets of the symmetry.

Theorem 21 (Symmetry of LSMs) *Given a dynamical system $\dot{x} = f(x)$ of the type (6) that fulfills the conditions of Theorem 32, and further given a symmetry (σ, τ) of $f(x)$ that fulfills Definition 9. Denote by \mathfrak{M} the Lyapunov subcenter manifold tangent to² the Eigenspace E_0 . If it holds that*

$$\sigma((\bar{Q}, 0)) = (\bar{Q}, 0), \quad (24)$$

and

$$E_0 = \sigma_* E_0, \quad (25)$$

then it also holds that

$$\mathfrak{M} = \sigma(\mathfrak{M}). \quad (26)$$

It also holds that any evolution $\gamma(\mathbb{R}) \in \mathfrak{M}$ satisfies

$$\gamma(\mathbb{R}) = \sigma(\gamma(\mathbb{R})). \quad (27)$$

PROOF. See Appendix A.4.

Remark 22 *In a local chart, condition (25) requires that E_0 is an eigenspace of the Jacobian $\frac{\partial S}{\partial x}|_{x=0}$.*

4.2 From LSMs to Eigenmanifolds

Here Theorem 32, Theorem 21 and the time-symmetry (15) are used to show that the LSMs of conservative mechanical systems are forced to fulfill definition 4.

First, apply Theorem 32 to the dynamic system (4) to verify the existence of unique LSMs at the stable equilibrium $(\bar{q}, 0)$. To the best knowledge of the authors, Theorem 23 is a minor contribution through its geometric (i.e., chart-free) formalism.

Theorem 23 (LSMs in mechanical systems)

Given the Hamiltonian dynamics (2) on $T^\mathcal{Q}$ with analytic Hamiltonian (1). If there is a point $\bar{Q} \in \mathcal{Q}$ where it holds that*

- (i) $dV(\bar{Q}) = 0$ and $\text{Hess}(V)(\bar{Q}) > 0$
- (ii) The $(0, 2)$ -tensor $M(\bar{Q})$ is positive definite and symmetric
- (iii) The $(1, 1)$ -tensor $M(\bar{Q})^{-1} \text{Hess}(V)(\bar{Q})$ is diagonalizable

² To be precise, with $\iota : \mathfrak{M} \rightarrow T^*\mathcal{Q}$ the natural embedding of \mathfrak{M} into $T^*\mathcal{Q}$, then \mathfrak{M} is tangent to E_0 if $\iota_* T_{(\bar{Q}, 0)} \mathfrak{M} \subset E_0$.

(iv) The eigenvalue $\lambda_0^2 = -\omega_0^2$ of $M(\bar{Q})^{-1}\text{Hess}(V)(\bar{Q})$ is non-resonant with the remaining eigenvalues λ_k , $1 \leq k \leq n-1$, which means that

$$\frac{\lambda_k^2}{\lambda_0^2} \notin \mathbb{Z}. \quad (28)$$

Then there exists, locally, a unique 2D submanifold $\mathfrak{M} \subset T^*\mathcal{Q}$ of periodic trajectories tangent to the eigenspace $E_0 = D_0 \oplus M(\bar{Q})D_0 \subset T_{(\bar{q},0)}T^*\mathcal{Q}$, where $D_0 = \ker(\omega_0^2 I - M(\bar{Q})^{-1}\text{Hess}(V)(\bar{Q}))$.

PROOF. See Appendix A.5.

Remark 24 When the non-resonance condition is not fulfilled, Lyapunov subcenter manifolds can still be found, but they are not unique [29].

The existence of a local Eigenmanifold is a novel result, that follows without further conditions:

Theorem 25 (Eigenmanifolds) *Given the conditions of Theorem 23, a neighborhood $\mathfrak{M}' \subset \mathfrak{M}$ of the equilibrium \bar{Q} is guaranteed to be an Eigenmanifold, and \mathfrak{M} is guaranteed to be a weak Eigenmanifold.*

PROOF. See Appendix A.6.

In other words, unique LSMs of conservative mechanical systems are weak Eigenmanifolds. A stronger, likewise novel version of Theorem 25 holds for the (restricted) class of systems with a 2D configuration manifold:

Theorem 26 (Eigenmanifolds) *Given the conditions of Theorem 23 for a conservative mechanical system with $\dim(\mathcal{Q}) = 2$, then \mathfrak{M} is guaranteed to be an Eigenmanifold.*

PROOF. See Appendix A.7. In other words, unique LSMs of 2D conservative mechanical systems are Eigenmanifolds. Finally, a lower bound for the number of Eigenmanifolds is a direct consequence of Corollary 33 and Theorem 25:

Corollary 27 (Number of Eigenmanifolds) *Consider a system of the type (4), with an equilibrium \bar{q} a minimum of the potential $V(q)$. If $m \leq n$ of the n eigenvalues ω_k^2 of the (1,1)-tensor $M(\bar{q})^{-1} \frac{\partial^2 V}{\partial q^T \partial q}(\bar{q})$ are mutually non-resonant, and non-resonant with the remaining eigenvalues, then there exist, locally, at least m unique Eigenmanifolds.*

4.3 From Eigenmanifolds to Rosenberg manifolds

Here, a sufficient condition is presented for Eigenmanifolds to fulfill the stronger properties of Rosenberg manifolds. These results follow from Theorem 25 together with 21, when the spatial symmetry 19 applies.

Theorem 28 (Rosenberg manifolds) *Given the conditions of Theorem 23, denoting \mathfrak{M} a weak Eigenmanifold and $\mathfrak{M}' \subset \mathfrak{M}$ an Eigenmanifold, both containing the equilibrium \bar{Q} of (4). If it holds that*

(i) $\varphi : \mathcal{M} \rightarrow \mathcal{M}$ exists such that $\varphi_*(\bar{Q}) = -id_{T_{\bar{Q}}\mathcal{Q}}$, and $\varphi \circ \varphi = id_{\mathcal{Q}}$, $V = V \circ \varphi$ and $M = \varphi^*M$

then there exists $\mathfrak{M}'' \subset \mathfrak{M}$ that is a weak Rosenberg Manifold. With $\mathfrak{M}' \subset \mathfrak{M}$ an Eigenmanifold, there also exists $\mathfrak{M}''' \subset \mathfrak{M}'$ that is a Rosenberg manifold. If it additionally holds that

(ii) \bar{Q} is the only fixed point of φ such that $V(\bar{Q}) \leq V(Q)$ for $Q \in \mathfrak{M}$

then equality holds, i.e., $\mathfrak{M}'' = \mathfrak{M}$ and $\mathfrak{M}''' = \mathfrak{M}'$.

PROOF. See Appendix A.8.

Remark 29 Recall that in φ -equivariant coordinates, Theorem 28 holds if $V(q) = V(-q)$ and $M(q) = M(-q)$.

5 Examples

This section presents two examples. The first example highlights various aspects of Theorems 26 and 28 for systems with $\dim(\mathcal{Q}) = 2$, to ease visual understanding. The second example is for $\dim(\mathcal{Q}) = 5$, and shows that the theoretical results apply to non-trivial systems.

5.1 Various 2-DoF systems

We consider the system of coupled masses in Fig. 2a, which is a Euclidean system with $\mathcal{M}_C = \mathbb{R}^2$ and a curvature-free metric tensor M_C given by

$$M_C(q) = \begin{bmatrix} m & 0 \\ 0 & m \end{bmatrix}, \quad (29)$$

and the double pendulum with parallel elasticity shown in Fig. 2b, which is a non-Euclidean system with $\mathcal{M}_{DP} = T^2$ and metric tensor M_{DP} given by

$$M_{DP}(q) = \begin{bmatrix} I + 3d^2m + 2d^2m \cos(q_2) & d^2m(1 + \cos(q_2)) \\ d^2m(1 + \cos(q_2)) & I + d^2m \end{bmatrix}. \quad (30)$$

We consider multiple choices of potential functions: two that are symmetric under (S_2, τ_2) for the presented chart, and one that is not symmetric. In particular, V_{s1} and V_a have similar terms, but the equilibrium of the spring for V_a is changed to $\pi/2$ such that $V_a(\bar{q} + q) \neq V_a(\bar{q} - q)$ for the minimum \bar{q} of V_a . V_{s2} is interesting because it results in an apparently "linear"

Table 2

Parameters for the example systems

Parameter	Value
m	0.4 kg
I	$1/12 \text{ kgm}^2$
d	1 m
k	10 Nm/rad
g	9.81 m/s^2

force, and highlights the importance of non-linearities in the inertia tensor.

$$V_{s1}(q) = 1/2k(q_2)^2 - dm g(2 \cos(q_1) + \cos(q_1 + q_2)),$$

$$V_{s2}(q) = 1/2kq_1^2 + 1/2k(q_2 - \pi/2)^2,$$

$$V_a(q) = 1/2k(q_2 - \pi/2)^2 - dm g(2 \cos(q_1) + \cos(q_1 + q_2)).$$

Parameters are chosen as summarized in Tab. 2.

We obtain a variety of systems by different pairings of the above metric tensors and potential functions, and denote a concrete system by a tuple (M, V) . In all combinations the dynamics are governed by (4). All systems satisfy the conditions of Theorem 26 for the existence of two unique Eigenmanifolds, and some satisfy the conditions of Theorem 28 for the existence of Rosenberg manifolds. This way, we put a particular focus on the implications of Theorem 28. The results from numerical continuation are summarized in Figs. 4, 5 and in Tab. 3. The case of (M_C, V_{s2}) is omitted since it is a linear system. As expected via Theorem 26, all systems show the existence of 2 Eigenmanifolds.

The double pendulum (M_{DP}, V_{s1}) with gravity and a spring at the second joint fulfills the conditions of 28, and shows families of geometric Rosenberg modes collected on generators. Example modes on its generators are shown in Fig. 4a & 4b. The double pendulum (M_{DP}, V_a) with asymmetric potential does not satisfy Theorem 28, such that there are no Rosenberg manifolds, although some modes on the remaining Eigenmanifolds are geometric Rosenberg modes. Examples of geometric eigenmodes are shown in Fig. 4d & 4e.

The double pendulum (M_{DP}, V_{s2}) with symmetric potential but asymmetric inertia tensor, also does not satisfy Theorem 28, and there are no Rosenberg manifolds. This is shown in Fig. 4f & 4g.

In the case of a (M_C, V_{s1}) , Theorem 28 holds and families of extended Rosenberg modes are found (or trivially, also for the linear system (M_C, V_{s2})). This is shown in Fig. 4h & 4i.

For the system (M_C, V_a) Theorem 28 does not hold, since the potential V_a is not symmetric about the equilibrium. Hence, Eigenmanifolds are found but Rosenberg manifolds are not. This highlights the existence of Eigenmanifolds for mechanical systems on Euclidean configuration manifolds that do not fall into the defini-

tion of [16, 17]. This is shown in Fig. 4j & 4k.

Finally, although Theorem 28 provides only a sufficient condition, we could not find any example of Rosenberg's manifolds for systems not fulfilling the hypotheses of Theorem 28. However, we observe that it is not uncommon to find isolated geometric Rosenberg modes. Indeed, these are not excluded by Theorem 28. This is highlighted by Fig. 5, which shows the minimum potential energy V along a given mode together with the energy of the starting point of that mode for all five systems. Whenever this minimum potential is zero, it the corresponding mode necessarily passes through the equilibrium. Thus, isolated zeros of this function identify isolated geometric Rosenberg modes within Eigenmanifolds.

5.2 Example of a high dimensional system

Let us now analyze the nonlinear normal modes of a more complex system satisfying the symmetry conditions required by Theorem 28. We take a quintuple pendulum as shown in Fig. 6 and set all masses to $m = 0.4\text{kg}$ and the link lengths $l = 1.0\text{m}$. For the potential, we use a diagonal stiffness matrix $K = 20I \frac{\text{Nm}}{\text{rad}}$ for a spring term and set $g = -9.81 \frac{\text{m}}{\text{s}^2}$. We do not report the full inertia tensor $M(q)$, but remark that $M(q) = M(-q)$ for q as chosen in Fig. 6.

The equilibrium configuration of the resulting system is found at $q = 0$, and eigenvalues of $M(0)^{-1} \frac{\partial^2 V}{\partial q \partial q}(0)$ are given by $(1123.58, 787.417, 255.266, 103.333, 56.6527)$, which are mutually non-resonant. Thus, Corollary 27 predicts the existence of 5 Eigenmanifolds. Our further aim is to numerically show that these are geometric Rosenberg manifolds, i.e., all modal oscillations pass through the equilibrium.

We start by computing the generators of the quintuple pendulum up to an energy level of $E_{max} = 100\text{J}$.

The lower triangular matrix in Fig. 7 shows the projections of the computed generators onto $q_i q_j$ -planes. For each generator, we highlight the configuration of maximal energy, which is indicated by the dots in the figure. We take these configurations as initial configuration and simulate the pendulum. This results in a periodic trajectory in form of a modal oscillation. The projected trajectory is shown in the upper triangular matrix in Fig. 7. All the oscillation pass, as predicted by Theorem 28 through the equilibrium in the center, and classify as geometric Rosenberg modes.

To achieve a better intuition on how the pendulum behaves we also show the generators and highest energy modal oscillation in Fig. 8. The equilibrium configuration of the pendulum is reached when all links are pointing straight downwards. Here, Theorem 28 implies that all modal oscillation pass through that configuration.

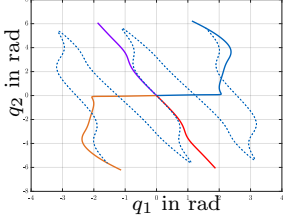
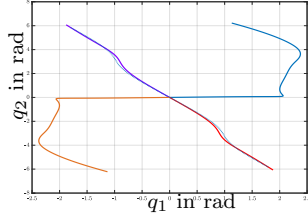
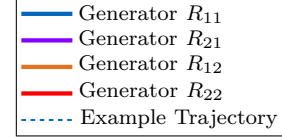
Although we have only shown the highest energy modal oscillation, the modal oscillation for all energy levels pass through the equilibrium.

Let us select, for instance, the fourth generator and look

Table 3

Summary of tested 2-DoF examples

System	System type	Potential	Inertia	Thm. 28 satisfied?	Figure
(M_{DP}, V_{s1})	non-Euclidean	Symmetric	Symmetric	✓	Fig. 4a, 4b
(M_{DP}, V_a)	non-Euclidean	Asymmetric	Symmetric	✗	Fig. 4d, 4e
(M_{DP}, V_{s2})	non-Euclidean	Symmetric	Asymmetric	✗	Fig. 4f, 4g
(M_C, V_{s1})	Euclidean	Symmetric	Symmetric	✓	Fig. 4h, 4i
(M_C, V_a)	Euclidean	Asymmetric	Symmetric	✗	Fig. 4j, 4k

(a) $(M_{DP}, V_{s1}), R_1$ (b) $(M_{DP}, V_{s1}), R_2$ 

(c) Legend

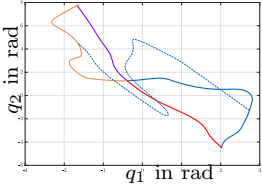
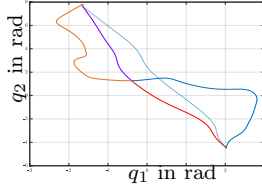
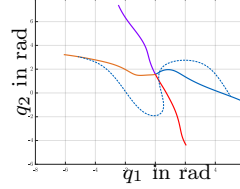
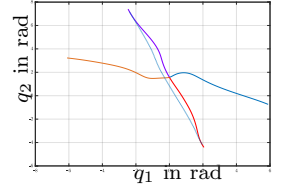
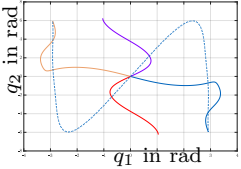
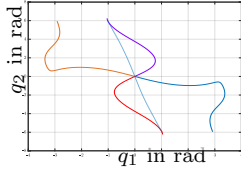
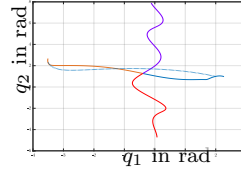
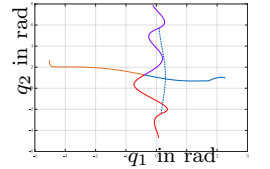
(d) $(M_{DP}, V_a), R_1$ (e) $(M_{DP}, V_a), R_2$ (f) $(M_{DP}, V_{s2}), R_1$ (g) $(M_{DP}, V_{s2}), R_2$ (h) $(M_C, V_{s1}), R_1$ (i) $(M_C, V_{s1}), R_2$ (j) $(M_C, V_a), R_1$ (k) $(M_C, V_a), R_2$

Figure 4. Results of numerical continuation for different example systems generated by combining different potential functions and inertia tensors. The solid lines show computed generators of the system. The pair of blue and orange solid lines show the two generators associated to the first Eigenmanifold and the pair of purple and red the two associated to the second Eigenmanifold. The dashed blue line shows an example modal oscillation of the system for one energy. The conditions states by Theorem 28 are satisfied for the cases (a,b) and (g,h).

at modal oscillations for various energy levels in Fig. 9. The left pane shows the initial configuration of the pendulum, while the right pane shows the trajectories of the point masses. Again, we observe that all modal oscillation pass through a configuration where all links point straight downwards.

6 Conclusion

Eigenmanifold theory connects to center manifold theory via Lyapunov subcenter manifolds, inheriting conditions for existence and uniqueness of Eigenmanifolds, and number of Eigenmanifolds about a given equilibrium. For conservative mechanical systems, we showed that non - resonance conditions guarantee that Lyapunov subcenter manifolds are unique and have the properties of weak Eigenmanifolds. When the config-

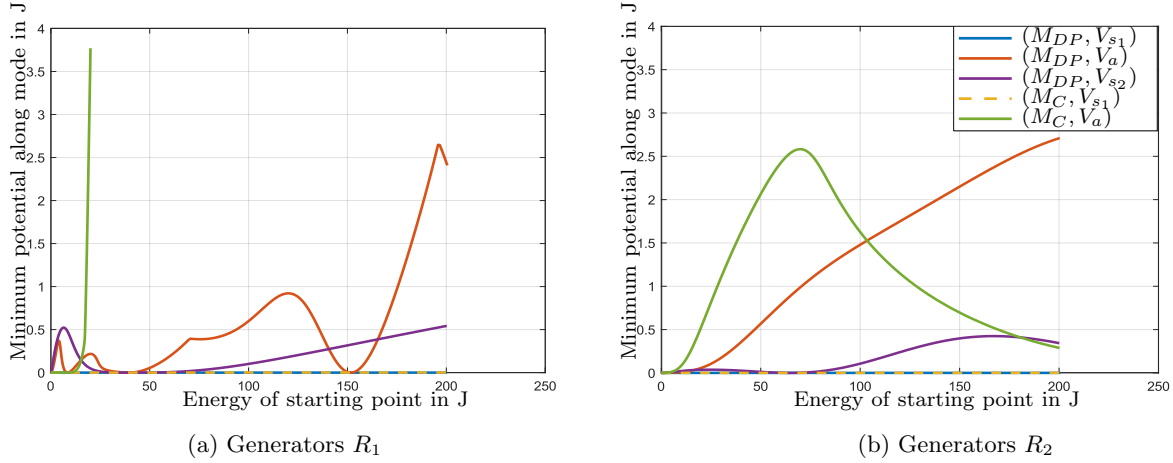


Figure 5. Minimal potential energy for modes of the example systems, split by modes collected on first and second generator.

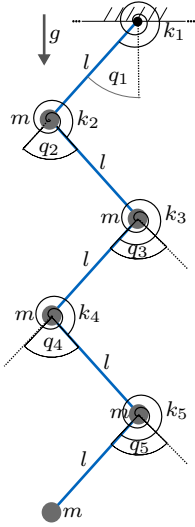


Figure 6. Quintuple Elastic Pendulum in Gravity Field

uration space is two - dimensional, unique Lyapunov subcenter manifolds are further guaranteed to be Eigenmanifolds. We presented a sufficient condition that results in unique Eigenmanifolds to fulfill the stronger properties of Rosenberg manifolds. In numerical examples, the absence of such continuous families was observed when these conditions were violated. The results confirm the validity of the presented Theorems, and the connection of Eigenmanifolds to the nonlinear dynamics literature enables future work on persistence of Eigenmanifolds under dissipative disturbances.

References

- [1] P. M. Wensing, J. Engelsberger, and J.-J. E. Slotine, “Coriolis factorizations and their connections to riemannian geometry,” 2023.
- [2] N. Jaquier and T. Asfour, “Riemannian geometry as a unifying theory for robot motion learning and control,” in *Robotics Research* (A. Billard, T. Asfour, and O. Khatib, eds.), (Cham), pp. 395–403, Springer Nature Switzerland, 2023.
- [3] B. P. J., H. Benjamin, M. B. J., K. N. J., and B. S. L., “Physics-informed dynamic mode decomposition,” *R. Soc. A*, 2023.
- [4] Y. Tong, H. Liu, and Z. Zhang, “Advancements in humanoid robots: A comprehensive review and future prospects,” *IEEE/CAA Journal of Automatica Sinica*, vol. 11, pp. 301–328, 2 2024.
- [5] G. Ficht and S. Behnke, “Bipedal humanoid hardware design: a technology review,” *Current Robotics Reports*, vol. 2, pp. 201–210, 6 2021.
- [6] H. Taheri and N. Mozayani, “A study on quadruped mobile robots,” *Mechanism and Machine Theory*, vol. 190, p. 105448, 2023.
- [7] M. Soori, B. Arezoo, and R. Dastres, “Optimization of energy consumption in industrial robots, a review,” *Cognitive Robotics*, vol. 3, pp. 142–157, 2023.
- [8] I. Dovgopolik and O. Borisov, “Simple energy-efficient path planning based on graph algorithms for articulated robotic-manipulators,” *IFAC-PapersOnLine*, vol. 56, no. 2, pp. 7014–7019, 2023. 22nd IFAC World Congress.
- [9] C. Della Santina and A. Albu-Schäffer, “Exciting Efficient Oscillations in Nonlinear Mechanical Systems Through Eigenmanifold Stabilization,” *IEEE Control Systems Letters*, vol. 5, pp. 1916–1921, Dec. 2021.
- [10] M. Raff, N. Rosa, and C. D. Remy, “Connecting gaits in energetically conservative legged systems,” *IEEE Robotics and Automation Letters*, 2022.
- [11] J. Cheng, Y. G. Alqaham, and Z. Gan, “Harnessing natural oscillations for high-speed, efficient asymmetrical locomotion in quadrupedal robots,” 2024.
- [12] J. I. Alora, M. Cenedese, E. Schmerling, G. Haller, and M. Pavone, “Data-driven spectral submanifold reduction for nonlinear optimal control of high-dimensional robots,” in *2023 IEEE International Conference on Robotics and Automation (ICRA)*, pp. 2627–2633, 2023.
- [13] V.-H. Vu, Z. Liu, and M. Thomas, “Flexible robot

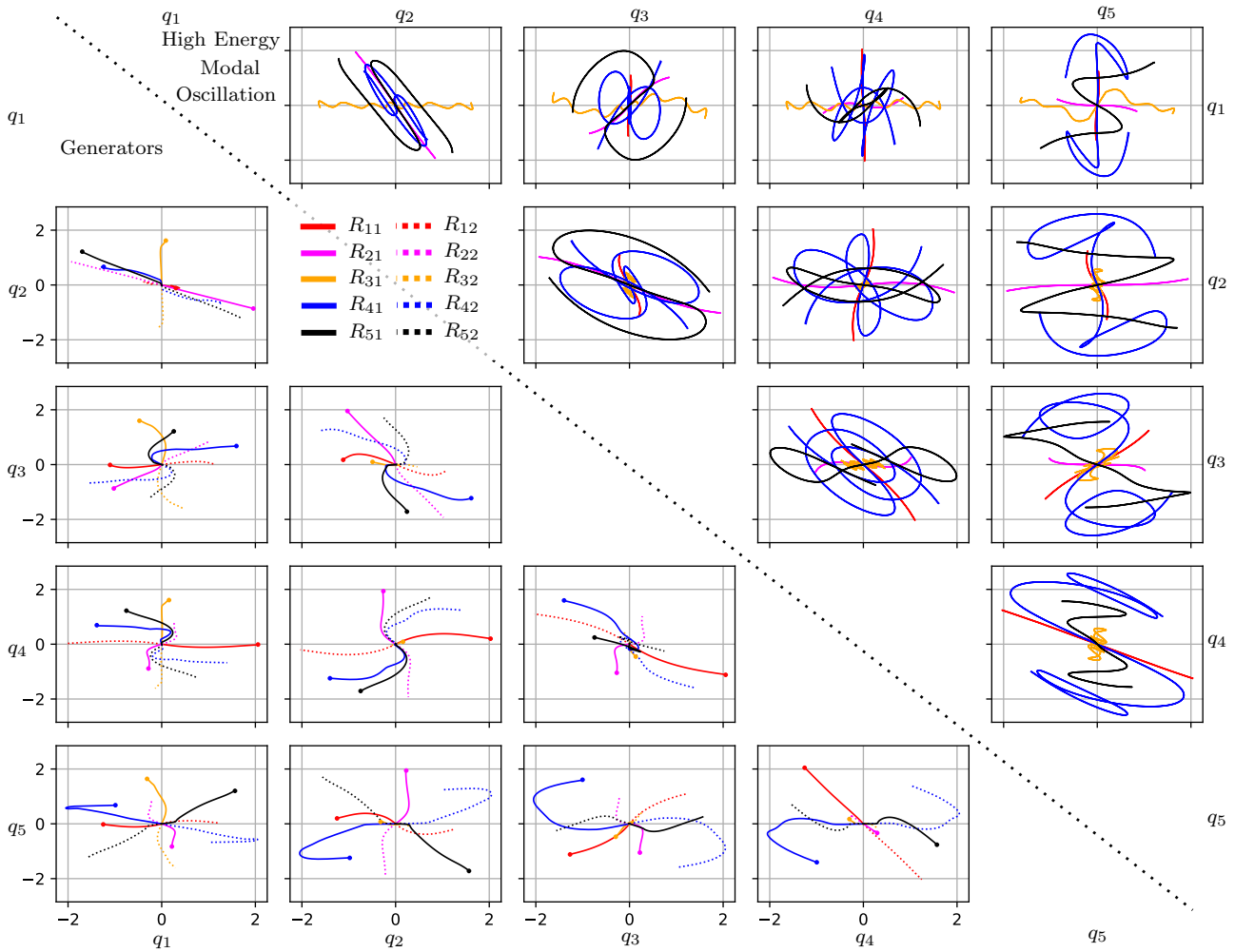


Figure 7. Generators and high energy modal oscillations of the quintuple pendulum shown in configuration space. The lower triangular matrix of plots shows the generators projected onto different $q_i q_j$ -planes. The upper triangular matrix of plots shows the corresponding modal oscillation for the highest energy on the color-matching generator. As the quintuple pendulum satisfies Theorem 28 all modal oscillations pass through the equilibrium. This is only shown for the highest energy oscillation, but the same is true for every other energy level.

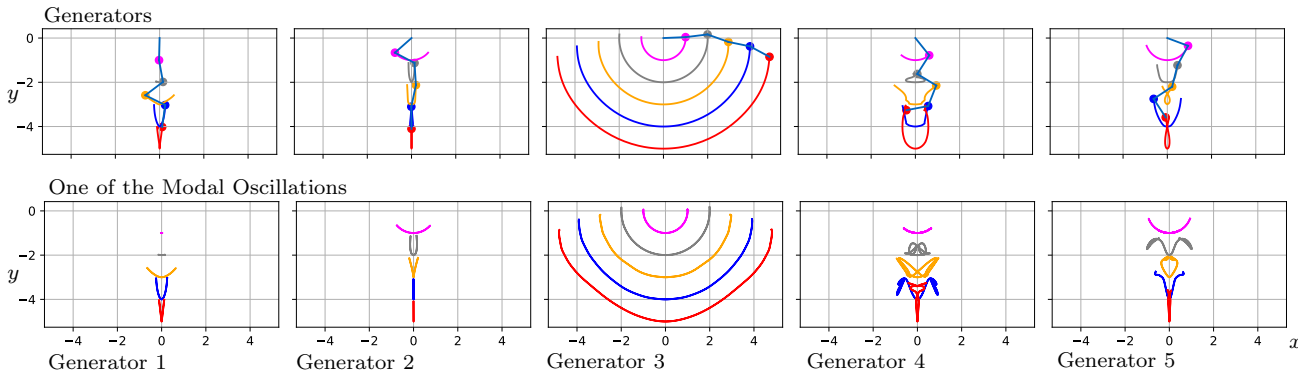


Figure 8. Cartesian version of Fig. 7. The top row shows the generators as Cartesian paths of the joints and the bottom row shows one modal oscillation. All of the modal oscillation pass through the equilibrium where all of the links of the pendulum point straight down.

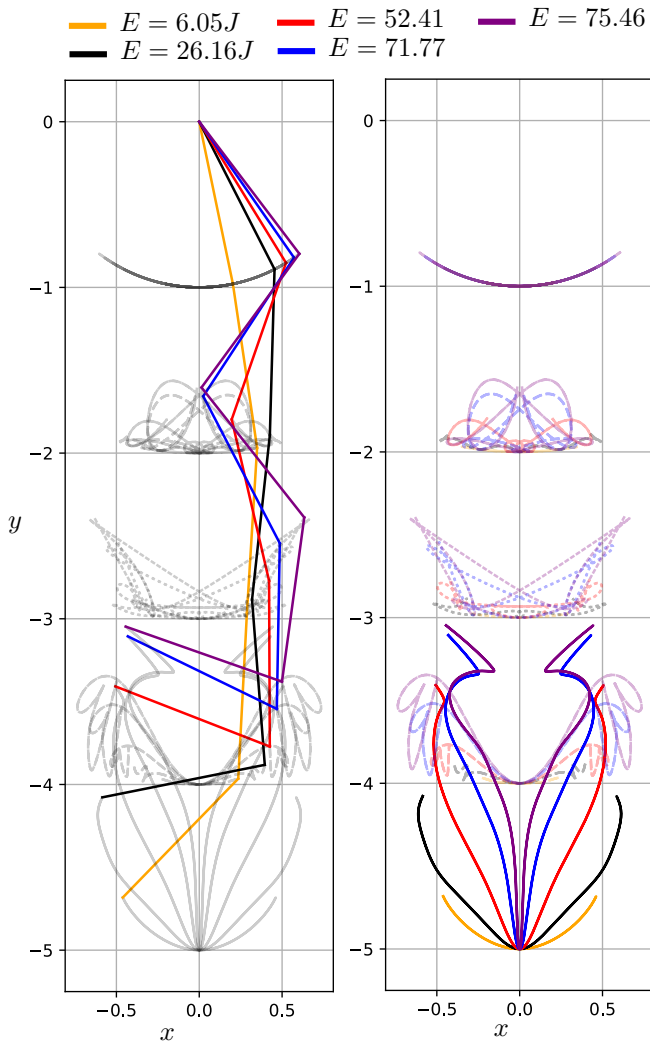


Figure 9. Modes with different energy levels for the fourth Eigenmanifold. The eigenmanifold is of the extended Rosenberg type. On the left the initial configurations are shown. On the right the modal oscillations of the tip are visualized in Cartesian space.

dynamics and vibration: From analytical modeling to operational modal analysis,” in *2024 10th International Conference on Automation, Robotics and Applications (ICARA)*, pp. 92–96, 2024.

[14] F. Bullo and A. D. Lewis, *Geometric Control of Mechanical Systems*, vol. 49 of *Texts in Applied Mathematics*. New York-Heidelberg-Berlin: Springer Science+Business Media New York, 2004.

[15] A. Albu-Schäffer and A. Sachtler, “What can algebraic topology and differential geometry teach us about intrinsic dynamics and global behavior of robots?,” *Springer Proceedings in Advanced Robotics*, vol. 27 SPAR, pp. 468–484, 2023.

[16] R. Rosenberg, “On nonlinear vibrations of systems with many degrees of freedom,” in *Advances in Applied Mechanics* (G. Chernyi, H. Dryden, P. Germain, L. Howarth, W. Olszak, W. Prager, R. Prob-

stein, and H. Ziegler, eds.), vol. 9 of *Advances in Applied Mechanics*, pp. 155 – 242, Elsevier, 1966.

[17] M. Peeters, R. Vigué, G. Sérandour, G. Kerschen, and J. C. Golinval, “Nonlinear normal modes, Part II: Toward a practical computation using numerical continuation techniques,” *Mechanical Systems and Signal Processing*, vol. 23, pp. 195–216, Jan. 2009.

[18] G. Kerschen, M. Peeters, J. C. Golinval, and A. F. Vakakis, “Nonlinear normal modes, part i: A useful framework for the structural dynamicist,” *Mechanical Systems and Signal Processing*, vol. 23, pp. 170–194, 1 2009.

[19] A. Albu-Schäffer and C. Della Santina, “A review on nonlinear modes in conservative mechanical systems,” *Annual Reviews in Control*, vol. 50, pp. 49 – 71, 2020.

[20] A. Sachtler, D. Calzolari, M. Raff, A. Schmidt, Y. P. Wotte, C. D. Santina, C. D. Remy, and A. Albu-Schäffer, “Swing-up of a weakly actuated double pendulum via nonlinear normal modes,” 4 2024.

[21] P. Pustina, D. Calzolari, A. Albu-Schäffer, A. D. Luca, and C. D. Santina, “Nonlinear modes as a tool for comparing the mathematical structure of dynamic models of soft robots,” pp. 779–785, 2 2024.

[22] A. Kelley and V. Sciences, “On the liapounov subcenter manifold,” *Journal of Mathematical Analysis and Applications*, vol. 18, pp. 472–478, 1967.

[23] C. Touzé, A. Vizzaccaro, and O. Thomas, “Model order reduction methods for geometrically nonlinear structures: a review of nonlinear techniques,” *Nonlinear Dynamics*, vol. 105, pp. 1141–1190, Jul 2021.

[24] S. Jain and G. Haller, “How to compute invariant manifolds and their reduced dynamics in high-dimensional finite element models,” *Nonlinear Dynamics*, vol. 107, pp. 1417–1450, Jan 2022.

[25] A. K. Stoychev and U. J. Römer, “Failing parametrizations: what can go wrong when approximating spectral submanifolds,” *Nonlinear Dynamics*, vol. 111, pp. 5963–6000, Apr 2023.

[26] J. Axås, B. Bäuerlein, K. Avila, and G. Haller, “Data-driven modeling of subharmonic forced response due to nonlinear resonance,” *Scientific Reports*, vol. 14, p. 25991, Oct 2024.

[27] M. Debeurre, S. Benacchio, A. Grolet, C. Grenat, C. Giraud-Audine, and O. Thomas, “Phase resonance testing of highly flexible structures: Measurement of conservative nonlinear modes and nonlinear damping identification,” *Mechanical Systems and Signal Processing*, vol. 215, p. 111423, 2024.

[28] M. Pozzi, J. Marconi, S. Jain, and F. Braghin, “Backbone curve tailoring via lyapunov subcenter manifold optimization,” *Nonlinear Dynamics*, vol. 112, pp. 15719–15739, Sep 2024.

[29] J. Sijbrand, “Properties of center manifolds,” *TRANSACTIONS OF THE AMERICAN MATHEMATICAL SOCIETY*, vol. 289, 1985.

[30] R. de la Llave, “Invariant manifolds associated to nonresonant spectral subspaces,” *Journal of Statis-*

tical Physics, vol. 87, 1997.

- [31] R. de la Llave and F. Kogelbauer, “Global persistence of Lyapunov-subcenter-manifolds as spectral submanifolds under dissipative perturbations,” 9 2018.
- [32] C. Della Santina, D. Calzolari, A. M. Giordano, and A. Albu-Schäffer, “Actuating Eigenmanifolds of Conservative Mechanical Systems via Bounded or Impulsive Control Actions,” *IEEE Robotics and Automation Letters*, vol. 6, pp. 2783–2790, Apr. 2021.
- [33] J. Moehlis and E. Knobloch, “Equivariant dynamical systems,” *Scholarpedia*, vol. 2, p. 2510, 2007.
- [34] J. Moyrón, J. Moreno-Valenzuela, and J. Sandoval, “Orbital stabilization for linear mechanical systems via a speed gradient algorithm,” in *2021 26th International Conference on Automation and Computing (ICAC)*, pp. 1–5, IEEE, 2021.
- [35] J. G. Romero and B. Yi, “Orbital stabilization of underactuated mechanical systems without Euler-Lagrange structure after of a collocated pre-feedback,” *arXiv preprint arXiv:2109.06724*, 2021.
- [36] C. F. Sætre, A. S. Shiriaev, L. B. Freidovich, S. V. Gusev, and L. M. Fridman, “Robust orbital stabilization: A Floquet theory-based approach,” *International Journal of Robust and Nonlinear Control*, vol. 31, no. 16, pp. 8075–8108, 2021.
- [37] G. Garofalo and C. Ott, “Passive energy-based control via energy tanks and release valve for limit cycle and compliance control,” *IFAC-PapersOnLine*, vol. 51, no. 22, pp. 73–78, 2018.
- [38] Z. Gan, Y. Yesilevskiy, P. Zaytsev, and C. D. Remy, “All common bipedal gaits emerge from a single passive model,” *Journal of The Royal Society Interface*, vol. 15, no. 146, p. 20180455, 2018.
- [39] N. Kashiri, A. Abate, S. J. Abram, A. Albu-Schäffer, P. J. Clary, M. Daley, S. Faraji, R. Furnemont, M. Garabini, H. Geyer, *et al.*, “An overview on principles for energy efficient robot locomotion,” *Frontiers in Robotics and AI*, vol. 5, p. 129, 2018.
- [40] N. Rosa and K. M. Lynch, “A topological approach to gait generation for biped robots,” *IEEE Transactions on Robotics*, vol. 38, no. 2, pp. 699–718, 2021.
- [41] R. Balderas Hill, S. Briot, A. Chriette, and P. Martinet, “Performing energy-efficient pick-and-place motions for high-speed robots by using variable stiffness springs,” *Journal of Mechanisms and Robotics*, pp. 1–12, 2021.
- [42] R. L. Hatton, Z. Brock, S. Chen, H. Choset, H. Faraji, R. Fu, N. Justus, and S. Ramasamy, “The geometry of optimal gaits for inertia-dominated kinematic systems,” *arXiv preprint arXiv:2102.01506*, 2021.
- [43] A. Seyfarth, “Template-based approach to resolve redundancies in motor control,” in *Novel Bioinspired Actuator Designs for Robotics*, pp. 21–25, Springer, 2021.
- [44] A. A. Biewener, R. J. Bompfrey, M. A. Daley, and A. J. Ijspeert, “Stability and manoeuvrability in animal movement: lessons from biology, modelling and robotics,” 2022.
- [45] J. Ding, P. Posthoorn, V. Atanassov, F. Boekel, J. Kober, and C. D. Santina, “Quadrupedal locomotion with parallel compliance: E-go design, modelling, and control,” 2024.
- [46] A. Sachtler and A. Albu-Schäffer, “Strict modes everywhere - bringing order into dynamics of mechanical systems by a potential compatible with the geodesic flow,” *IEEE Robotics and Automation Letters*, vol. 7, pp. 2337–2344, 4 2022.
- [47] Y. P. Wotte, S. Dummer, N. Botteghi, C. Brune, S. Stramigioli, and F. Califano, “Discovering efficient periodic behaviors in mechanical systems via neural approximators,” *Optimal Control Applications and Methods*, vol. 44, pp. 3052–3079, 2023.
- [48] C. D. Santina, D. Calzolari, A. M. Giordano, and A. Albu-Schäffer, “Actuating eigenmanifolds of conservative mechanical systems via bounded or impulsive control actions,” *IEEE Robotics and Automation Letters*, vol. 6, pp. 2783–2790, 4 2021.
- [49] C. D. Santina and A. Albu-Schäffer, “Exciting efficient oscillations in nonlinear mechanical systems through eigenmanifold stabilization,” *IEEE Control Systems Letters*, vol. 5, pp. 1916–1921, 12 2021.
- [50] F. Bjelonic, A. Sachtler, A. Albu-Schäffer, and C. D. Santina, “Experimental closed-loop excitation of nonlinear normal modes on an elastic industrial robot,” *IEEE Robotics and Automation Letters*, vol. 7, pp. 1689–1696, 4 2022.
- [51] A. Coelho, A. Albu-Schäffer, A. Sachtler, H. Mishra, D. Bicego, C. Ott, and A. Franchi, “Eigenmpc: An eigenmanifold-inspired model-predictive control framework for exciting efficient oscillations in mechanical systems,” *Proceedings of the IEEE Conference on Decision and Control*, vol. 2022-December, pp. 2437–2442, 2022.
- [52] C. D. Santina, D. Lakatos, A. Bicchi, and A. Albu-Schäffer, “Using nonlinear normal modes for execution of efficient cyclic motions in articulated soft robots,” *Springer Proceedings in Advanced Robotics*, vol. 19, pp. 566–575, 2021.
- [53] Y. V. Mikhlin, T. V. Shmatko, and G. V. Manucharyan, “Lyapunov definition and stability of regular or chaotic vibration modes in systems with several equilibrium positions,” *Computers & Structures*, vol. 82, pp. 2733–2742, 12 2004.
- [54] Y. Mikhlin and K. V. Avramov, “Nonlinear normal modes of vibrating mechanical systems: 10 years of progress,” *Applied Mechanics Reviews*, vol. 76, pp. 1–57, 9 2023.
- [55] K. V. Avramov and Y. V. Mikhlin, “Review of Applications of Nonlinear Normal Modes for Vibrating Mechanical Systems,” *Applied Mechanics Reviews*, vol. 65, Apr. 2013.
- [56] A. Albu-Schäffer, D. Lakatos, and S. Stramigioli, “Strict nonlinear normal modes of systems characterized by scalar functions on riemannian man-

ifolds,” *IEEE Robotics and Automation Letters*, vol. 6, pp. 1910–1917, 4 2021.

- [57] A. Vanderbauwhede and G. Iooss, “Center manifold theory in infinite dimensions,” pp. 125–163, 1992.
- [58] M. Field, “Dynamics and symmetry,” 2007.
- [59] A. K. Mishra and M. C. Singh, “The normal modes of non-linear symmetric systems by group representation theory,” *International Journal of Non-Linear Mechanics*, vol. 9, pp. 463–480, 12 1974.
- [60] G. M. Chechin, V. P. Sakhnenko, H. T. Stokes, A. D. Smith, and D. M. Hatch, “Non-linear normal modes for systems with discrete symmetry,” *International Journal of Non-Linear Mechanics*, vol. 35, pp. 497–513, 5 2000.
- [61] J. S. W. Lamb and J. A. G. Roberts, “Time-reversal symmetry in dynamical systems: A survey,” *Physica D: Nonlinear Phenomena*, vol. 112, pp. 1–39, Jan. 1998.
- [62] R. Alomair and J. Montaldi, “Periodic Orbits in Hamiltonian Systems with Involutory Symmetries,” *Journal of Dynamics and Differential Equations*, vol. 29, pp. 1283–1307, Dec. 2017.
- [63] H. Gluck and W. Ziller, “Existence of periodic motions of conservative systems,” *Seminar on Minimal Submanifolds*, pp. 65–98, 1983.
- [64] J. M. Lee, *Introduction to Smooth Manifolds*. Springer New York, NY, 2 ed., 2012.
- [65] R. Abraham and J. E. Marsden, *Foundations of Mechanics, Second Edition*. Addison-Wesley Publishing Company, Inc., 1987.

A Proofs

A.1 Proof of Theorem 6

We prove the following theorem:

Theorem 6 (Existence of generator) *Given a smooth Eigenmanifold \mathfrak{M} that satisfies Definition 4, the set $\mathcal{R} := \{(Q, 0) \mid (Q, 0) \in \mathfrak{M}\}$ is a connected, 1D submanifold containing the equilibrium and $\mathfrak{M} = \Psi_{X_H}^{\mathbb{R}}(\mathcal{R})$, i.e., \mathcal{R} generates \mathfrak{M} .*

PROOF. We first show that $\mathcal{R} = \{(Q, 0) \mid (Q, 0) \in \mathfrak{M}\}$ is a regular 1-dimensional submanifold of \mathfrak{M} . We use the regular level set theorem [64, Corr. 5.24], which states that $\mathcal{R} \subset \mathfrak{M}$ is a closed, embedded submanifold of dimension 1 if there is a function $\alpha : \mathfrak{M} \rightarrow \mathbb{R}$ such that $\mathcal{R} = \alpha^{-1}(0)$ and $\text{Im}(d\alpha) = T_0\mathbb{R}$. To this end, note that

$$\alpha(Q, P) = M^{-1}(dV(Q), P) + M^{-1}(P, P). \quad (\text{A.1})$$

is as required. Indeed, the generator is marked by the requirement that $P = 0$, which corresponds to $\alpha(Q, 0) = 0$. For $\text{Im}(d\alpha) = T_0\mathbb{R}$, consider that \mathfrak{M} is tangent to the flow X_H , and apply $d\alpha(Q, P)$ to the tangent vector

$X_H(Q, P)$ at $(Q, 0) \in \mathfrak{M}$:

$$\begin{aligned} d\alpha(X_H) &= M^{-1}(dV(Q), \dot{P}) \\ &= M^{-1}(dV(Q), dV(Q)) \neq 0. \end{aligned} \quad (\text{A.2})$$

Thus, it follows from the regular level set theorem [64] that \mathcal{R} is indeed a closed, embedded 1D submanifold. This holds where $dV(Q) \neq 0$, i.e., at all points other than the equilibrium. The equilibrium itself may be included as a limit point, since geometric eigenmodes arbitrarily close to $(Q, 0)$ may be found by definition of \mathfrak{M} .

Since there are two points of $P = 0$ per geometric eigenmode, and \mathfrak{M} only consists of geometric eigenmodes and the equilibrium, it necessarily holds that $\mathfrak{M} = \Psi_{X_H}^{\mathbb{R}}(\mathcal{R})$.

From the closedness of \mathcal{R} it can be shown that it is connected:

Consider ”polar” coordinates $X : \mathfrak{M} \rightarrow \mathbb{R}^2$, such that orbits are mapped to lines of constant radius, and angle θ ranges from 0 to 2π over a full oscillation. Then submanifolds of the generator are open sets parameterized as

$$\mathcal{R}_{0,i} = (r_i(x), \theta_i(x)). \quad (\text{A.3})$$

By Lemma 13, there is a second generator

$$\sigma_1(\mathcal{R}_{0,i}) = (r_i(x), -\theta_i(x)). \quad (\text{A.4})$$

Since every orbit is ”generated” by \mathcal{R} , any r must be reached for some r_i . The closed intervals $\mathcal{R}_{0,i}$ must simultaneously exist on isolated orbits. Yet, if $\mathcal{R}_{0,i}, \mathcal{R}_{0,j}, \sigma_1(\mathcal{R}_{0,i})$ and $\sigma_1(\mathcal{R}_{0,j})$ are distinct for a given r , there would have to be geometric eigenmodes with at least four points of $P = 0$. This is not possible. Thus, the requirement that any r is on the generator means that the generator must be connected.

A.2 Time symmetry and spatial symmetry

For ease of readability, time-symmetry of conservative mechanical systems is proven in canonical coordinates (see also Appendix B.2).

Theorem 30 (Time symmetry) *If $x(t) = (q(t), p(t))$ is a solution of the dynamics (4), then $y(t) = (q(-t), -p(-t))$ is also a solution.*

PROOF. This follows directly from application of Theorem 10, if it can be shown that (13) is a symmetry of (4). To this end, denote

$$F(x) = \begin{pmatrix} M(q)^{-1}p \\ -\frac{\partial}{\partial q}(p^\top M(q)^{-1}p) - \frac{\partial V}{\partial q}(q) \end{pmatrix} \quad (\text{A.5})$$

Then it has to be shown that

$$\tau_1 \frac{\partial S_1}{\partial x} F(x) = F(S_1(x)). \quad (\text{A.6})$$

For the right-hand side

$$F(S_1(x)) = F(q, -p) = \begin{pmatrix} -M(q)^{-1}p \\ -\frac{\partial}{\partial q}(p^\top M(q)^{-1}p) - \frac{\partial V}{\partial q}(q) \end{pmatrix}.$$

For the left-hand side

$$\begin{aligned} \tau_1 \frac{\partial S_1}{\partial x} F(x) &= \begin{bmatrix} -I & 0 \\ 0 & I \end{bmatrix} F(x) \\ &= \begin{pmatrix} -M(q)^{-1}p \\ -\frac{\partial}{\partial q}(p^\top M(q)^{-1}p) - \frac{\partial V}{\partial q}(q) \end{pmatrix}. \end{aligned} \quad (\text{A.7})$$

This completes the proof.

The spatial symmetry of conservative mechanical systems is stated in φ -equivariant coordinates (see also Appendix B.4).

Theorem 31 (Spatial symmetry) *If $M(q) = M(-q)$, $V(q) = V(-q)$, and $x(t) = (q(t), p(t))$ is a solution of the dynamics (4), then $y(t) = (-q(t), -p(t))$ is also a solution.*

PROOF. This follows directly from application of Theorem 10, if it can be shown that (19) is a symmetry of (4). To this end, denote

$$F(x) = \begin{pmatrix} M(q)^{-1}p \\ -\frac{\partial}{\partial q}(p^\top M(q)^{-1}p) - \frac{\partial V}{\partial q}(q) \end{pmatrix} \quad (\text{A.8})$$

Then it has to be shown that

$$\frac{\partial S_2}{\partial x} F(x) = F(S_2(x)). \quad (\text{A.9})$$

Note that the gradient of an even function $h(q) = h(-q)$ is odd, i.e., $\frac{\partial h}{\partial q}(q) = -\frac{\partial h}{\partial q}(-q)$. Further, both the kinetic and potential energy are even in q . Thus the right-hand side is

$$\begin{aligned} F(S_2(x)) &= F(-q, -p) \\ &= \begin{pmatrix} -M(-q)^{-1}p \\ -1/2 \frac{\partial}{\partial s}(p^\top M(s)^{-1}p)_{s=-q} - \frac{\partial V}{\partial s}_{s=-q} \end{pmatrix} \\ &= \begin{pmatrix} -M(q)^{-1}p \\ \frac{\partial}{\partial q}(p^\top M(q)^{-1}p) + \frac{\partial V}{\partial q} \end{pmatrix}. \end{aligned} \quad (\text{A.10})$$

For the left-hand side

$$\begin{aligned} \tau_1 \frac{\partial S_2}{\partial x} F(x) &= \begin{bmatrix} -I & 0 \\ 0 & -I \end{bmatrix} F(x) \\ &= \begin{pmatrix} -M(q)^{-1}p \\ \frac{\partial}{\partial q}(p^\top M(q)^{-1}p) + \frac{\partial V}{\partial q}(q) \end{pmatrix}. \end{aligned} \quad (\text{A.11})$$

This completes the proof.

A.3 Proofs of Lemmas and Corollaries

We state here proofs for Lemmas 13, 16 and 18, and Corollaries 15 and 20.

A.3.1 Lemma 13

Lemma 13 *Given an evolution $\gamma(t) = (Q(t), P(t))$ of (2). If there are two distinct points $(Q_1, 0), (Q_2, 0) \in \gamma(\mathbb{R})$ and denoting $\Delta t = \min\{t > 0 \mid (Q_2, 0) = \Psi_{X_H}^t(Q_1, 0)\}$, then the evolution is periodic with period $T = 2\Delta t$.*

PROOF. Without loss of generality, let $\gamma(0) = (Q_1, 0)$ and $\gamma(\Delta t) = (Q_2, 0)$. Let $\gamma_1(t) = (Q(t), P(t))$ and $\gamma_2(t) = \sigma_1 \gamma_1(\tau_1 t) = (Q(-t), -P(-t))$. Then

$$\gamma_1(0) = (Q_1, 0), \quad (\text{A.12})$$

$$\gamma_2(0) = (Q_1, 0), \quad (\text{A.13})$$

and it follows from uniqueness of solutions that $\gamma_1(t) = \gamma_2(t)$. It also holds that

$$\gamma_1(\Delta t) = (Q_2, 0), \quad (\text{A.14})$$

$$\gamma_2(-\Delta t) = (Q_2, 0). \quad (\text{A.15})$$

Since $\gamma_1(-\Delta t) = \gamma_1(\Delta t)$, the evolution must be periodic. Since Δt is minimal, this period must be $T = 2\Delta t = 2|t' - t''|$.

A.3.2 Corollary 15

Corollary 15 *Given $T > 0$, a T -periodic orbit $\gamma(t)$ is a weak geometric eigenmode if and only if it satisfies the symmetry*

$$\gamma(\mathbb{R}) = \sigma_1(\gamma(\mathbb{R})). \quad (\text{A.16})$$

PROOF. If: given the symmetry, Theorem 12a guarantees a point with $P(t') = 0$. Then periodicity and Theorem 12b guarantee that a second point with $P(t' + T/2) = 0$ is encountered. Then the segment is such that

$$Q([t', t' + T/2]) = Q([t' + T/2, t' + T]). \quad (\text{A.17})$$

Additionally, it holds that $\phi_\gamma(s) = \pi_Q(\gamma(2(t' + t)/T))$ is an immersion that maps the interval $[0, 1]$ to $Q([t', t' +$

$T/2]$). Since, $Q([t', t' + T/2]) = Q([t' + T/2, t' + T])$, this extends to $\pi_{\mathcal{Q}}(\gamma(\mathbb{R}))$, and $\gamma(t)$ is a weak geometric eigenmode.

Only if: a weak geometric eigenmode necessarily encounters two points with $P(t) = 0$, such that the symmetry is satisfied as a consequence of Theorem 12.

A.3.3 Lemma 16

Lemma 16 *Given an evolution $\gamma(t) = (Q(t), P(t))$ of (2). If there is a pair of points $(Q, P), (\varphi(Q), \varphi^{-1*}P) \in \gamma(\mathbb{R})$ and denoting $\Delta t = \min\{t > 0 \mid (\varphi(Q), \varphi^{-1*}P) = \Psi_{X_H}^t((Q, P))\}$, then the evolution is periodic with period $T = 2\Delta t$ and*

$$\gamma(\mathbb{R}) = \sigma_2(\gamma(\mathbb{R})). \quad (\text{A.18})$$

PROOF. Let $\gamma_1(t) = (Q(t), P(t))$ be a solution to the equations of motion (4). Via (19)

$$\gamma_2(t) = (\varphi(Q)(t), \varphi^{-1*}P(t)), \quad (\text{A.19})$$

must also be a solution. By hypothesis, the points $\gamma_1(0) = (Q, P)$ and $\gamma_2(0) = (\varphi(Q), \varphi^{-1*}P)$ lie on the same trajectory, and

$$\gamma_1(\Delta t) = \gamma_2(0). \quad (\text{A.20})$$

Similarly $\gamma_2(\Delta t) = \gamma_1(0)$, such that $\gamma_1(2\Delta t) = \gamma_2(\Delta t) = \gamma_1(0)$, i.e., $\gamma(t)$ is periodic and $T = 2\Delta t$ is the period, since Δt is minimal. It also follows from A.20 that $\gamma_1(t + T/2) = \gamma_2(t)$, which yields

$$Q(t + T/2) = \varphi(Q(t)) \quad (\text{A.21})$$

$$P(t + T/2) = \varphi^{-1*}P(t). \quad (\text{A.22})$$

I.e., for any $(Q, P) \in \gamma(\mathbb{R})$ it also holds that $(\varphi(Q), \varphi^{-1*}P) \in \gamma(\mathbb{R})$, which concludes the proof.

A.3.4 Lemma 18

Lemma 18 *Given an evolution $\gamma(t) = (Q(t), P(t))$ of (2). If there is a pair of points $(Q, 0), (\varphi(Q), 0) \in \gamma(\mathbb{R})$ then $\nu \in \mathbb{R}^n$ exists such that $(\mathfrak{q}, \nu) \in \gamma(\mathbb{R})$, with $\mathfrak{q} = \varphi(\mathfrak{q})$.*

PROOF. By use of Lemma 13, $\gamma(t)$ is periodic and without loss of generality, $\gamma(0) = (Q, 0)$ and $\gamma(T/2) = (\varphi(Q), 0)$. Through the symmetry (σ_1, τ_1) , equation (16) holds and in particular

$$Q(T/4) = Q(-T/4). \quad (\text{A.23})$$

Through the symmetry (σ_2, τ_2) , equation (A.21) holds and in particular

$$Q(T/4) = \varphi(Q(-T/4)). \quad (\text{A.24})$$

Combining (A.23) and (A.24) yields

$$Q(-T/4) = \varphi(Q(-T/4)), \quad (\text{A.25})$$

i.e., $Q(t)$ is guaranteed to move through a fixed point $\mathfrak{q} = Q(-T/4)$ of $\varphi : \mathcal{Q} \rightarrow \mathcal{Q}$.

A.3.5 Corollary 20

Corollary 20 *Given $T > 0$, a T -periodic orbit $\gamma(t)$ is a weak geometric Rosenberg mode if it satisfies the symmetries*

$$\gamma(\mathbb{R}) = \sigma_1(\gamma(\mathbb{R})) = \sigma_2(\gamma(\mathbb{R})). \quad (\text{A.26})$$

If the fixed point \bar{Q} of σ_1, σ_2 is the only fixed point such that $V(\bar{Q}) < V(Q)$ for $(Q, 0) \in \gamma(\mathbb{R})$, then $\gamma(t)$ is a weak geometric Rosenberg mode w.r.t. \bar{Q} .

PROOF. For $\gamma(t)$ to be a weak geometric Rosenberg mode, it is required that it is a weak geometric eigenmode and that $\mathfrak{q} \in \pi_{\mathcal{Q}}(\gamma(\mathbb{R}))$ for some equilibrium $(\mathfrak{q}, 0)$ of the dynamics X_H .

By Corollary 15, $\gamma(t)$ that satisfies $\gamma(\mathbb{R}) = \sigma_1(\gamma(\mathbb{R}))$ is necessarily a weak geometric eigenmode.

By Lemma 18, $\gamma(t)$ that additionally satisfies $\gamma(\mathbb{R}) = \sigma_2(\gamma(\mathbb{R}))$ necessarily contains a fixed point \mathfrak{q} , and by [33], such \mathfrak{q} is necessarily an Equilibrium. Hence, $\gamma(t)$ is a weak geometric Rosenberg mode w.r.t. \mathfrak{q} .

However, it is also known that $V(\mathfrak{q}) < V(Q)$ for an endpoint $(Q, 0)$ of the mode $\gamma(t)$. If $\mathfrak{q} = \bar{Q}$ is the only such candidate, $\gamma(t)$ is necessarily a weak Rosenberg mode passing through \bar{Q} .

A.4 Proof of Theorem 21

Theorem 21 (Symmetry of LSMs) *Given a dynamical system $\dot{x} = f(x)$ of the type (6) that fulfills the conditions of Theorem 32, and further given a symmetry (σ, τ) of $f(x)$ that fulfills Definition 9. Denote by \mathfrak{M} the Lyapunov subcenter manifold tangent to³ the Eigenspace E_0 . If it holds that*

$$\sigma((\bar{Q}, 0)) = (\bar{Q}, 0), \quad (\text{A.27})$$

and

$$E_0 = \sigma_* E_0, \quad (\text{A.28})$$

then it also holds that

$$\mathfrak{M} = \sigma(\mathfrak{M}). \quad (\text{A.29})$$

³ To be precise, with $\iota : \mathfrak{M} \rightarrow T^*\mathcal{Q}$ the natural embedding of \mathfrak{M} into $T^*\mathcal{Q}$, then \mathfrak{M} is tangent to E_0 if $\iota_* T_{(\bar{Q}, 0)}\mathfrak{M} \subset E_0$.

It also holds that any evolution $\gamma(\mathbb{R}) \in \mathfrak{M}$ satisfies

$$\gamma(\mathbb{R}) = \sigma(\gamma(\mathbb{R})). \quad (\text{A.30})$$

PROOF. Begin by showing that $\mathfrak{M} = \sigma(\mathfrak{M})$. The presence of the symmetry σ implies that both \mathfrak{M} and $\mathfrak{M}' := \sigma(\mathfrak{M})$ are LSMs, and condition $\sigma(0) = 0$ implies that $0 \in \mathfrak{M}$ and $0 \in \mathfrak{M}'$, i.e., both are LSMs about the equilibrium $x = 0$. Further, $\sigma_* E_0 = E_0$ implies that both \mathfrak{M} and \mathfrak{M}' are tangent to the eigenspace E_0 . Theorem 23 holds, such that \mathfrak{M} is the unique LSM tangent to E_0 , and hence it must be that $\mathfrak{M} = \mathfrak{M}'$.

To show that also $\gamma(\mathbb{R}) = \sigma(\gamma(\mathbb{R}))$, introduce coordinates (U, X) on \mathfrak{M} , i.e., $U \subset \mathfrak{M}$ is a neighborhood of $x = 0$ and $X : \mathfrak{M} \rightarrow \mathbb{R}^2$. Further, choose "polar" coordinates X and a time scaling $\tau : \mathfrak{M} \rightarrow \mathbb{R}_+$ such that $X(\gamma(t)) = (r, t)$ with r constant for a given oscillation $\gamma \in \mathfrak{M}$. Then $\sigma : \mathfrak{M} \rightarrow \mathfrak{M}$ translates into coordinates as

$$S(r, t) = (\alpha(r), t + c), \quad (\text{A.31})$$

Since it must map solutions to solutions. The condition

$$\sigma \circ \sigma = \text{id}_{\mathfrak{M}}, \quad \sigma(0) = 0 \quad (\text{A.32})$$

translates into coordinates as

$$S(S(r, \theta)) = (r, \theta), \quad \Phi(0, \theta) = 0, \quad (\text{A.33})$$

or in terms of α

$$\alpha(\alpha(r)) = r, \quad \alpha(0) = 0, \quad (\text{A.34})$$

With the additional constraint that $\alpha(r) \geq 0$, this has the unique continuous solution $\alpha(r) = r$. Thus

$$S(r, t) = (r, t + c), \quad (\text{A.35})$$

necessarily maps solutions into themselves, i.e., $\sigma(\gamma(\mathbb{R})) = \gamma(\mathbb{R})$, completing the proof.

A.5 Proof of Theorem 23

We begin by stating a coordinate-based version of Theorem 23, assuming only the existence of a local canonical chart (see Appendix B.2) that maps the equilibrium \bar{Q} to $q = \bar{q}$. We prove this chart-version, and subsequently remark on its chart invariance.

Theorem 23 (LSMs in mechanical systems) *If it holds that*

- (i) $(q, p) = (\bar{q}, 0)$ is a stable equilibrium, i.e., $\frac{\partial V}{\partial q}(\bar{q}) = 0$ and $\frac{\partial^2 V}{\partial q^2}(\bar{q}) > 0$.

(ii) $M(\bar{q})$ is positive definite and symmetric

(iii) $M(\bar{q})^{-1} \frac{\partial^2 V}{\partial q \partial q}(\bar{q})$ is diagonalizable

(iv) The eigenvalue $\lambda_0^2 = -\omega_0^2$ of $M(\bar{q})^{-1} \frac{\partial^2 V}{\partial q \partial q}(\bar{q})$ is non-resonant with the remaining eigenvalues λ_k , $1 \leq k \leq n-1$, i.e.,

$$\frac{\lambda_k^2}{\lambda_0^2} \notin \mathbb{Z}. \quad (\text{A.36})$$

Then there exists, locally, a unique 2D submanifold $\mathfrak{M} \subseteq \mathbb{R}^{2n}$ of periodic trajectories tangent to the eigenspace spanned by $E_{\pm} = \ker(\pm i\omega_0 I - A)$.

PROOF. Given the conditions of Theorem 23, we are going to show that the conditions for Theorem 32 are fulfilled. This guarantees the existence and uniqueness of a local Lyapunov subcenter manifold.

First, we express the Hamiltonian dynamics of a mechanical system (4) in an arbitrary canonical chart with coordinates (q, p) such that the equilibrium $(\bar{Q}, 0)$ is mapped to $q = \bar{q}$, $p = 0$. Further write $x = (q, p) \in \mathbb{R}^{2n}$. The dynamics then take the form

$$\dot{x} := f(x) = \begin{pmatrix} M(q)^{-1} p \\ -\frac{\partial}{\partial q}(p^\top M(q)^{-1} p) - \frac{\partial V}{\partial q}(q) \end{pmatrix}, \quad (\text{A.37})$$

which can be rewritten as

$$\dot{x} = Ax + B(x), \quad (\text{A.38})$$

with $x = (q - \bar{q}, p)$ a change to another canonical chart and

$$A = \frac{\partial f}{\partial x}((\bar{q}, 0)) = \begin{bmatrix} 0 & M(\bar{q})^{-1} \\ -\frac{\partial^2 V}{\partial q \partial q}(\bar{q}) & 0 \end{bmatrix}, \quad (\text{A.39})$$

$$B(x) = f(x) - Ax. \quad (\text{A.40})$$

The dynamics are of the required form (6) for Theorem 32, since $B(0) = 0$, and $\frac{\partial B}{\partial x}(0) = 0$. $B(x)$ is also analytic, given that $M(q), V(q)$ are analytic. This does not rely on the choice of a particular chart: the matrix A is coordinate invariant, given that $dV(\bar{q}) = 0$, which follows from $(\bar{q}, 0)$ being an equilibrium of the dynamics (4).

The eigenvalues λ of $A = \begin{bmatrix} 0 & B \\ C & 0 \end{bmatrix}$ are the solution to

$$\det(\lambda I_{2n} - A) = \det(\lambda^2 I_n - BC) = 0, \quad (\text{A.41})$$

such that A is diagonalizable since the $(1, 1)$ -tensor $BC = -M(\bar{q})^{-1} \frac{\partial^2 V}{\partial q \partial q}(\bar{q})$ is diagonalizable. Thus, condition (i) of Theorem 32 is fulfilled.

Further, $\lambda^2 = -\omega^2$ for some positive $\omega \in \mathbb{R}_+$, since $M(\bar{q})^{-1} \frac{\partial^2 V}{\partial q \partial q}(\bar{q})$ is a positive definite matrix, and eigenvalues $-\omega_j^2$ of $-M(\bar{q})^{-1} \frac{\partial^2 V}{\partial q \partial q}(\bar{q})$ correspond to pairs of eigenvalues

$$\lambda_{j,\pm} = \pm i\omega_j \quad (\text{A.42})$$

of A . Thus, condition (ii) of Theorem 32 is fulfilled.

The eigenvalues $\lambda_{0,\pm}$ are non-resonant with the remaining $2n - 2$ eigenvalues $\lambda_{k,\pm}$ of A , since

$$\frac{\lambda_k^2}{\lambda_{0,\pm}^2} \notin \mathbb{Z} \Rightarrow \frac{\lambda_k}{\lambda_{0,\pm}} \notin \mathbb{Z}, \quad (\text{A.43})$$

where $\frac{\lambda_k^2}{\lambda_{0,\pm}^2} \notin \mathbb{Z}$ is guaranteed by assumption. Thus, also condition (iii) of Theorem 32 is fulfilled.

Finally, note that the existence of a conserved quantity $H(x(t))$ fulfilling condition (iv) of Theorem 32 is given by the Hamiltonian $H(x(t)) = \frac{1}{2}p^\top M(q)^{-1}p + V(q)$.

No specific chart was assumed, and the conditions of Theorem 23 are chart-invariant: the equilibrium is guaranteed to be of the form $(\bar{q}, 0)$ in any canonical chart, $M(q)$ is positive definite and symmetric in any chart, and eigenvalues of the $(1, 1)$ -tensor $M(\bar{q})^{-1} \frac{\partial^2 V}{\partial q \partial q}(\bar{q})$ are chart-invariant. Indeed, expressing these conditions in their chart-invariant form leads to Theorem 23.

A.6 Proof of Theorem 25

Theorem 25 (Weak Eigenmanifolds) *Given the conditions of Theorem 23, a neighborhood $\mathfrak{M}' \subset \mathfrak{M}$ of the equilibrium \bar{Q} is guaranteed to be an Eigenmanifold, and \mathfrak{M} is guaranteed to be a weak Eigenmanifold.*

PROOF. Note that the symmetry (S_1, τ_1) satisfies the conditions of Theorem 21:

$$S_1((0, 0)) = (0, 0), \quad (\text{A.44})$$

and the eigenspace $E_0 := D \oplus M(\bar{Q})D$ is such that

$$E_0 = \frac{\partial S_1}{\partial x} E_0 = \begin{bmatrix} I & 0 \\ 0 & -I \end{bmatrix} E_0. \quad (\text{A.45})$$

Hence, the LSM \mathfrak{M} is necessarily such that

$$\mathfrak{M} = \sigma_1(\mathfrak{M}), \quad (\text{A.46})$$

$$\gamma(\mathbb{R}) = \sigma_1(\gamma(\mathbb{R})). \quad (\text{A.47})$$

By Corollary 15, the trajectories $\gamma(\mathbb{R})$ are weak geometric eigenmodes. Since the limiting behavior of $\gamma(t) = \Psi_f^t(\gamma_0) \in \mathcal{M}_0$ as $\gamma_0 = (Q, 0)$ approaches $(\bar{Q}, 0)$ is that

of a linear eigenmode, which necessarily does not self-intersect, there must also be a neighborhood $\mathfrak{M}'_0 \subset \mathfrak{M}$ where evolutions do not self-intersect and thus classify as geometric eigenmodes, making \mathfrak{M}'_0 an eigenmanifold.

Remark 30 *The proof breaks down if $\mathfrak{M} \neq \sigma(\mathfrak{M})$, such as could be the case if the family \mathcal{M}_0 bifurcates into multiple 2D collections of periodic orbits, further away from the equilibrium.*

A.7 Proof of Theorem 26

Theorem 26 (Eigenmanifold) *Given the conditions of Theorem 23 for a conservative mechanical system with $\dim(\mathcal{Q}) = 2$, then \mathfrak{M} is guaranteed to be an Eigenmanifold.*

PROOF. Following the argumentation of A.6, start with the existence of a neighborhood $\mathfrak{M}'_0 \subset \mathfrak{M}$ that contains geometric eigenmodes. If the oscillations self-intersect in \mathfrak{M} , one of two scenarios must occur in transitioning from \mathfrak{M}' to \mathfrak{M} (see also Figures A.1a and A.1b). A unique LSM necessarily collects weak geometric eigenmodes, and we show that these transitions are not weak geometric eigenmodes, making them impossible.

Scenario a, a first order intersection where either Q_1 or Q_2 passes through another Q contained within $\pi_{\mathcal{Q}}(\gamma(\mathbb{R}))$. Since $V(Q_1) = V(Q_2) > V(Q)$ present a strict upper bound for $V(Q)$ of any other point on the eigenmode. A first order intersection would imply e.g., $V(Q) = V(Q_2)$ and by conservation of energy the momentum at Q must be 0. Thus point $(Q_2, 0)$ is encountered twice in a given period, which is not possible for a non-equilibrium solution.

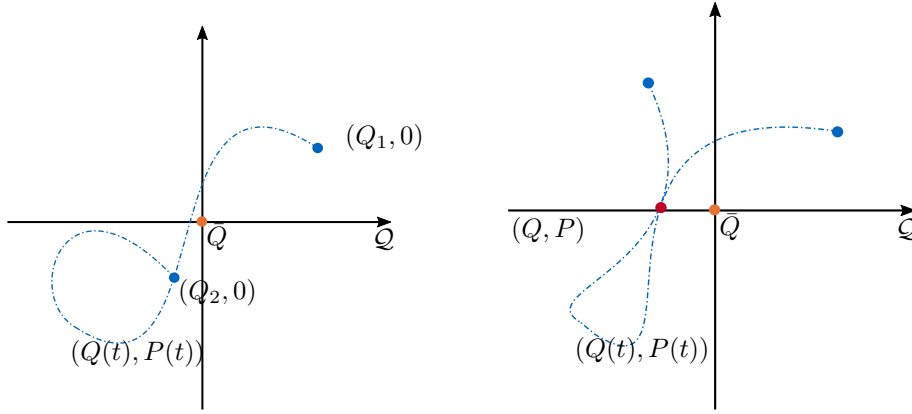
Scenario b, a second higher order intersection where $\gamma(\mathbb{R})$ is tangent to itself at some point $(Q, P) \in \gamma(\mathbb{R})$. Uniqueness of solutions forbids this transition, since the system must have a unique solution through any (Q, P) .

Remark 31 *The proof breaks down for higher dimensions, since other first order intersections are possible that do not require Q_1 or Q_2 to pass through another Q . However, we reason that self-intersections are a $\text{Codim}(n - 1)$ phenomenon and become less "likely" with increasing n , being most common for $\dim(\mathcal{Q}) = 3$.*

A.8 Proof of Theorem 28

Theorem 28 (Rosenberg manifolds) *Given the conditions of Theorem 23, denoting \mathfrak{M} a weak Eigenmanifold and $\mathfrak{M}' \subset \mathfrak{M}$ an Eigenmanifold, both containing the equilibrium \bar{Q} of (4). If it holds that*

- (i) $\varphi : \mathcal{M} \rightarrow \mathcal{M}$ exists such that $\varphi_*(\bar{Q}) = -id_{T_{\bar{Q}}\mathcal{Q}}$, and $\varphi \circ \varphi = id_{\mathcal{Q}}$, $V = V \circ \varphi$ and $M = \varphi^* M$



(a) First order self-intersection of a geometric eigenmode.

(b) Higher order self-intersection of a geometric eigenmode.

Figure A.1. Possible self-intersections of Eigenmodes along a generator, in a mechanical system with two dimensional configuration space. In transitioning from a geometric eigenmode to a weak geometric eigenmode, either (a) a first order intersection takes places or (b) a higher order intersection takes place. However, a unique LSM necessarily contains weak geometric eigenmodes (Theorem 25), and neither scenario is a valid weak geometric eigenmode, such that these transitions are impossible.

then there exists $\mathfrak{M}'' \subset \mathfrak{M}$ that is a weak Rosenberg Manifold. With $\mathfrak{M}' \subset \mathfrak{M}$ an Eigenmanifold, there also exists $\mathfrak{M}''' \subset \mathfrak{M}'$ that is a Rosenberg manifold. If it additionally holds that

- (ii) \bar{Q} is the only fixed point of φ such that $V(\bar{Q}) \leq V(Q)$ for $Q \in \mathfrak{M}$

then equality holds, i.e., $\mathfrak{M}'' = \mathfrak{M}$ and $\mathfrak{M}''' = \mathfrak{M}'$.

PROOF. By Theorems 23 and 25 the weak Eigenmanifold \mathfrak{M} and the Eigenmanifold $\mathfrak{M}' \subset \mathfrak{M}$ exist and are unique. \mathfrak{M} , \mathfrak{M}' , and trajectories on either are by definition subject to the symmetry (S_1, τ_1) . By condition 1., the symmetry (S_2, τ_2) applies to the dynamics (4), such that Theorem 21 guarantees that $\mathfrak{M}, \mathfrak{M}'$ and trajectories on either are subject to this symmetry, too. Thus, it holds that

$$\mathfrak{M} = S_1(\mathfrak{M}) = S_2(\mathfrak{M}), \quad (\text{A.48})$$

$$\mathfrak{M}' = S_1(\mathfrak{M}') = S_2(\mathfrak{M}'), \quad (\text{A.49})$$

$$\gamma(\mathbb{R}) = S_1(\gamma(\mathbb{R})) = S_2(\gamma(\mathbb{R})). \quad (\text{A.50})$$

Since the potential is locally convex about the equilibrium \bar{Q} , it holds that $V(\bar{Q}) < V(Q)$ in a neighborhood of \bar{Q} . The point \bar{Q} is also a fixed point of the symmetry S_2 , so the condition of Corollary 20 applies, within a neighborhood of \bar{Q} , so a neighborhood $\mathfrak{M}'' \subset \mathfrak{M}$ must consist of weak Rosenberg modes and a neighborhood $\mathfrak{M}''' \subset \mathfrak{M}'$ must consist of Rosenberg modes.

By addition of condition 2., Corollary 20 is satisfied globally, i.e., a unique fixed point \bar{Q} exists such that $V(\bar{Q}) < V(Q)$ for all $(Q, 0)$ in \mathfrak{M} . Then all weak Eigenmodes in \mathfrak{M} are weak Rosenberg modes, and all Eigenmodes in \mathfrak{M}' are Rosenberg modes.

B Additional Material

B.1 Lyapunov subcenter manifolds

We briefly introduce Lyapunov subcenter manifolds (LSMs), focusing on applications to systems of the type (4). For a complete treatment, refer to de la Llave et al. [31, 30] and references therein.

For the general description of LSMs, focus on the class of dynamical system on $\mathcal{M} = \mathbb{R}^{2n}$ that is given by

$$\dot{x} = Ax + B(x), \quad (\text{B.1})$$

with $x \in \mathbb{R}^{2n}$, $A \in \mathbb{R}^{2n \times 2n}$ and analytic $B : \mathbb{R}^{2n} \rightarrow \mathbb{R}^{2n}$ such that $B(0) = 0$, $\frac{\partial B}{\partial x}(0) = 0$.

Denote as $(\lambda_1, \dots, \lambda_{2n})$ the eigenvalues of A , and denote by $E_k = \ker(\lambda_k I - A) \subset \mathbb{C}^{2n}$ the linear eigenspace associated with λ_k .

We repeat [31, Ass. 2.1 & Thm. 2.5] of de la Llave et al. on the existence and uniqueness of LSMs:

Theorem 32 (Lyapunov subcenter manifolds) *If it holds that*

- (i) A is diagonalizable.
- (ii) A has a pair of conjugate eigenvalues $\pm i\omega_0$ with zero real part.
- (iii) The remaining $2n - 2$ eigenvalues λ_k of A , with $1 \leq k \leq 2n - 2$, are non-resonant with the eigenvalues $\pm i\omega_0$, i.e. it holds for all k that

$$\frac{\lambda_k}{i\omega_0} \notin \mathbb{Z}. \quad (\text{B.2})$$

(iv) The system (B.1) has a conserved quantity $H(x(t))$ along integral curves $x(t)$, i.e.,

$$\frac{d}{dt}H(x(t)) = 0. \quad (\text{B.3})$$

Further, $H(0) = 0$, $(\frac{\partial}{\partial x}H)(0) = 0$, and

$$Y^\top \left(\left(\frac{\partial^2}{\partial x \partial x^\top} H \right) (0) \right) Y > 0, \forall Y \in E_0,$$

with E_0 the eigenspace associated with $\pm i\omega_0$.

Then there exists, locally, a unique 2D submanifold $\mathfrak{M} \subseteq \mathbb{R}^{2n}$ of periodic trajectories tangent to the eigenspace E_0 of $\pm i\omega_0$.

We call this 2D submanifold \mathfrak{M} the Lyapunov subcenter manifold associated with the eigenspace E_0 at $x = 0$. It follows by repeated application of Theorem 32:

Corollary 33 *If d of the n pairs of eigenvalues $\pm i\omega_k$ of A , $1 \leq k \leq n$, are mutually non-resonant, and non-resonant with the remaining eigenvalues, then there exist, locally, at least d unique families of periodic orbits, with a unique family being tangent to a given eigenspace E_k of A .*

Corollary 33 merely provides a lower bound since the conditions of Theorem 32 are sufficient, but not necessary.

B.2 Canonical charts on $T^*\mathcal{Q}$

Define coordinates on \mathcal{Q} by a chart (U, X) with $U \subset \mathcal{Q}$ and $X : U \rightarrow \mathbb{R}^n$, assigning coordinates to $Q \in \mathcal{Q}$ by

$$(q_1, \dots, q_n) := X(Q). \quad (\text{B.4})$$

At the point Q , this induces a fibre-wise chart $(T_Q^*\mathcal{Q}, X^{-1*})$ via the pullback $X^{-1*} : T_Q^*\mathcal{Q} \rightarrow \mathbb{R}^n$ that assigns to $P \in T_Q^*\mathcal{Q}$ the coordinates

$$(p_1, \dots, p_n) = X^{-1*}(P). \quad (\text{B.5})$$

A canonical chart on $T^*U \subset T^*\mathcal{Q}$ then assigns to $(Q, P) \in T^*U$ the coordinates $(q_1, \dots, q_n, p_1, \dots, p_n)$.

B.3 The geometric Hessian of a function

Denote by $d : C^\infty(\mathcal{M}) \rightarrow \Gamma(T^*\mathcal{M})$ the differential of a function and by $\nabla \cdot : \Gamma(T\mathcal{M}) \times \Gamma(T_q^p\mathcal{M}) \rightarrow \Gamma(T_q^p\mathcal{M})$ the covariant derivative w.r.t. a given connection on \mathcal{M} . The Hessian of $V \in C^2(\mathcal{M}, \mathbb{R})$ is defined as

$$\text{Hess}(V)(X, Y) := (\nabla_X dV)(Y). \quad (\text{B.6})$$

In a local chart we denote $dV = \frac{\partial V}{\partial x^j} dx^j$, write $X = X^i \frac{\partial}{\partial x^i}$, $Y = Y^i \frac{\partial}{\partial x^i}$, and the choice of connection corresponds to a choice of Christoffel Symbols Γ_{ij}^k . Using Einstein summation notation, the Hessian reads

$$\text{Hess}(V)(X, Y) = X^j \frac{\partial^2 V}{\partial x^i \partial x^j} Y^i - X^j \frac{\partial V}{\partial x^k} \Gamma_{ij}^k Y^i. \quad (\text{B.7})$$

At points $m \in \mathcal{M}$ where $dV = 0$, we have that

$$\text{Hess}(V) = \frac{\partial^2 V}{\partial x^i \partial x^j} dx^i dx^j, \quad (\text{B.8})$$

i.e., $\text{Hess}(V)(X, Y)$ is a $(0, 2)$ -tensor at critical points of V , and is then also independent of the choice of Christoffel symbols Γ_{ij}^k .

B.4 Equivariant coordinates

Given an diffeomorphism $\varphi : \mathcal{Q} \rightarrow \mathcal{Q}$, that leaves an equilibrium $\bar{Q} \in \mathcal{Q}$ fixed, satisfies that $\varphi_*(\bar{q}) = -\text{id}_{T_{\bar{q}}\mathcal{Q}}$ and $\varphi \circ \varphi = \text{id}_{\mathcal{Q}}$.

Pick any chart (U, X) with chart-region $\bar{Q} \in U \subset \mathcal{Q}$ and (diffeomorphic) chart-map $X : \mathcal{Q} \rightarrow \mathbb{R}^n$. We want to find a chart (V', Y) such that $S_2(q, p) = (-q, -p)$. For this it is sufficient that $Y \circ \varphi \circ Y^{-1}(q) = -q$, or equivalently

$$Y \circ \varphi = -Y. \quad (\text{B.9})$$

Define a candidate chart (V, Y) by

$$V := \{Q \in U \mid \varphi(Q) \in U\}, \quad (\text{B.10})$$

$$Y := \frac{1}{2}(X - X \circ \varphi). \quad (\text{B.11})$$

Then the coordinate description of the symmetry is $Y \circ \varphi(Q) = -Y(Q)$, as desired. Also note that V is well defined since $\varphi \circ \varphi = \text{id}_{\mathcal{Q}}$.

It remains to be shown that Y is a valid chart-map, i.e., that Y is a local diffeomorphism. This follows from the inverse function theorem [65, Theorem 1.3.12] by showing that $Y_*(\bar{Q})$ is full rank:

$$Y_*(\bar{Q}) = \frac{1}{2}(X_*(\bar{Q}) - X_*(\bar{Q})\varphi_*(\bar{Q})) = X_*(\bar{Q}). \quad (\text{B.12})$$

Here, the first step uses that $\varphi(\bar{Q}) = \bar{Q}$ and the second step uses that $\varphi_*(\bar{q}) = -\text{id}_{T_{\bar{q}}\mathcal{Q}}$. This is indeed full rank, since X is itself a local diffeomorphism. Thus, a neighborhood $V' \subset V$ of \bar{Q} exists such that (V', Y) is a valid chart with the desired properties.